Regulation of neurotransmitter release by C-domain Ca²-sensors

Bourgeois-Jaarsma, Q.

2020

Chapter 1

1

Chapter 1

General Introduction

This thesis focuses on two different aspects of presynaptic mechanisms related to the regulation of neurotransmission. On one hand, it deals with presynaptic Ca^{2+} signaling and on the other hand with various Ca^{2+}-sensing proteins, known as C_2 domain proteins. Altogether, the general aim is to provide new insight in the presynaptic mechanisms regulating neurotransmitter release, from the regulation of Ca^{2+} event generation to the control of synaptic vesicle fusion by various Ca^{2+} sensors.

Neurons communicate with each other over long distances through axonal projections that conduct electrical signals. Highly arborized dendritic projections and cell bodies (somata) receive signals from presynaptic boutons of other neurons. Electrical activity in neurons is controlled by a negative resting membrane potential, which results from a net negative charge in the cytoplasm relative to the extracellular space. Due to the activity of selective ion channels, pumps and exchangers, various ions (e.g. Na^+, K^+, Ca^{2+} and Cl^-) exhibit very different concentrations in and outside living neurons. Voltage sensitive channels are activated by changes in the membrane potential to (selectively) conduct aforementioned ions. The interplay of multiple such processes can lead to the generation of action potentials (APs) which are propagated along the axonal plasma membrane in an all-or-none manner [1].

1. The synapse: elementary unit of information processing

The brain is the most complex organ within the human body. It is composed of an extremely intricate network composed of around (~) 100 billion neurons and around 10 times more glial cells [2,3] to support, protect and modulate their functions. Each neuron can form up to 1000 connections or synapses, the number varying greatly between neuronal subtypes. The resulting ~100 trillion synapses altogether enable motor control, learning, memory and higher-level cognitive functions such as decision making. Chemical synapses (Figure 1) opposed to electrical synapses represent the majority of neuronal inter-connections in the central nervous system and they compose the elementary unit necessary for information transmission between neurons. They are the intercellular junction between a presynaptic neuron and a postsynaptic cell.

The synaptic vesicle cycle

The presynaptic release site contains vesicles which are synthesized *de novo* or are rapidly and locally recycled to the active zone (AZ), a protein dense structure where they are secreted (Figure 1). Newly formed vesicles originate from the trans-Golgi network [4].

In the synapse they accumulate and store neurotransmitters at high concentrations [5]. To achieve this, a vacuolar proton pump [6] first establishes a proton gradient across the vesicle membrane, resulting in the acidification of the vesicle lumen [7,8]. The proton gradient subsequently drives neurotransmitter loading into the vesicle lumen [8]. The tethering of synaptic vesicles close to voltage-gated Ca^{2+} channels (VGCCs) is mediated by presynaptic scaffolding proteins associated to the presynaptic plasma membrane in the active zone. Important scaffolding proteins include Piccolo, RIM and ELKS, among others [9–11] (for review [12,13]). The precise arrangement of VGCCs, vesicles and protein components of the release machinery ensures rapid and efficient neurotransmitter secretion during presynaptic depolarization.

Upon electrical stimulation, the action potential triggers the fusion of the synaptic vesicle membrane and the plasma membrane, which leads to the release of neurotransmitters into the synaptic cleft (Figure 1). The neurotransmitters then bind to receptors on the postsynaptic surface, typically causing them to open and conduct ion currents (so called ionotropic receptors). The excitatory neurotransmitter glutamate binds to AMPA (α-amino-3-hydroxy-5-methyl-4-isoxazolepropionic acid) and NMDA (*N*-methyl-D-aspartate) receptors, leading to depolarization of the postsynaptic neuron. The inhibitory neurotransmitter GABA (gamma-aminobutyric acid) binds to $GABA_A$ receptors and induces hyperpolarization through influx of Cl^- ions.

1.1. Organization and function of the presynaptic release site

For many synapses, especially those which transmit sensory information at high frequencies such as the Calyx of Held [14] or retinal ribbon synapses [15], information transfer reliability is of key importance. This requires the maintenance of a sufficient ready releasable pool (RRP) size. The trafficking of synaptic vesicles (SVs) is highly organized by many proteins associated or interacting with them [16]. Different types of synapses employ different molecular architectures, synaptic vesicle pools and produce diverse release kinetics triggered by distinct physiological signals.

Vesicle pools

Different definitions can be used to identify vesicle pools. The mainstream definition is based on electrophysiological studies reporting functional vesicle release properties. Alternatively, a morphological approach is used to distinguish docked and non-docked vesicles by electron microscopy [17,18]. Morphological approaches however cannot distinguish docked vs. primed vesicles. Biochemical methods aspire to define distinct groups of vesicles based on molecular markers. Vesicular docking is supported by both morphological and biochemical evidence. Yet, the functional role of synaptic docking remains elusive. Recent studies have investigated the influence of the number and occupancy of docking sites on neurotransmission using functional methods [17,18] (see review [19]). Taking benefit of 'simple synapses', single synaptic contacts in the cerebellum which contain a single active zone and postsynaptic density, local Ca^{2+} uncaging was used to obtain direct measurements of the readily releasable vesicle pool (RRP). This procedure established that each synaptic contact contains a fixed number of docking sites [20]. A related investigation used the same structure

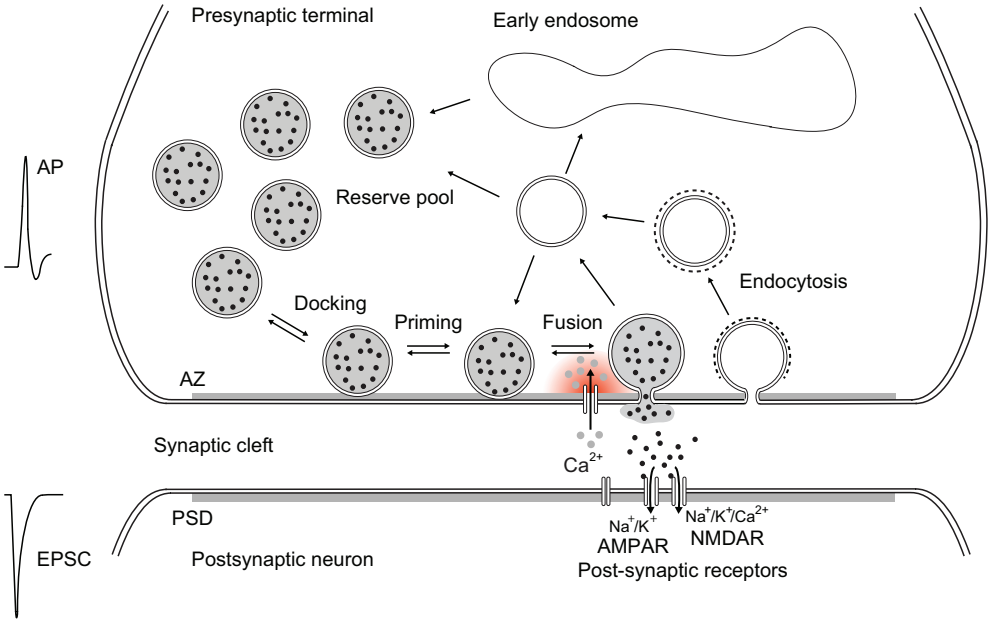

Figure 1. The synaptic vesicle cycle. Overview of vesicle trafficking at a glutamatergic synapse. First, neurotransmitters are actively transported into synaptic vesicles, which cluster in front of the active zone to form the reserve pool. Vesicles then dock at the active zone (AZ), where they are primed to convert them into a state of competence for Ca^{2+}-triggered fusion-pore opening. Upon electrical stimulation and concomitant Ca^{2+} influx, vesicles fuse with the plasma membrane and release their content in the synaptic cleft. After full fusion, the vesicle membrane and most of its associated proteins are endocytosed and return to the endosome for recycling. Alternatively, vesicles may in some cases be retrieved by a kiss-and-run process. After its release, glutamate activates postsynaptic AMPA and NMDA receptors, generating an excitatory postsynaptic current (EPSC) which depolarizes the postsynaptic neuron. If the depolarization is sufficient, this causes the generation of an action potential in the postsynaptic neuron. The synaptic release probability (Pr) is the average probability that a presynaptic active zone releases one or more vesicles following an action potential. It depends on the vesicular release probability (P_{vr}) and the number of vesicles in the pool and determines the synaptic reliability.

to estimate the number of docking site per synapse and the variety between synapses of the same type, based on failure statistics. A correlation could be made between the variations of docking sites and the signal transmission, in terms of release probability and synaptic plasticity [17]. At excitatory synapses, synaptic release probability was calculated to match single release sites. This mathematic transformation, combined with Ca^{2+}-imaging enabled to estimate the occupancy of docking sites [18].

The substantial gap that existed between functional (primed vesicles) versus structural analysis (morphologically docked vesicles) has also been addressed using novel imaging techniques. High-pressure freezing and high resolution electron microscopy (EM) immediately after photostimulation enabled to visualize the nanoscale organization of synaptic vesicles in correlation with functional neurotransmitter release [19,20]. Functional EM enabled to detect vesicle pool dynamics during synaptic transmission and suggests that

docked vesicle pool and RRP are partially overlapping [21]. Another application of the flash-and freeze technique also argues for the idea that docking and priming cannot be stricly separated by showing that a mutant variant which impairs synchronous release compromised the attachment of synaptic vesicles to the plasma membrane [22,23]. At hippocampal mossy fibers, flash-and-freeze experiments demonstrated that synaptic potentiation is primarily caused by an increase in the RRP, unraveling the correlation between structural vesicle dynamic and presynaptic plasticity [24].

In our we use the electrophysiological definition, where vesicle pools have been segregated into three distinct pools: the reserve or resting pool, the recycling pool (RP) and the RRP [25–29]. The reserve pool is a depot of synaptic vesicles from which the discharge is initiated only after 10 to 15 seconds of intense stimulation [27,29]. It constitutes the majority of vesicles in presynaptic terminals (~85%, around 180 vesicles per synapse in hippocampal neuron culture) [25,27,30] and may have a minor contribution during physiological activity [25,28]. Reserve pool vesicles classically considered as rather static could be exchanged with the recycling pool on a long time scale [31] possibly after the induction of potentiation [32]. A part of this pool could also undergo recycling even at rest. The turnover dynamics of the reserve pool are difficult to assess. A rough estimate indicates that turnover occurs slowly after cessation of tetanic stimulation [33], with a time constant of several minutes [27,31,34]. The recycling pool (10% and around 20 vesicles) maintains release during moderate stimulation [25,28]. Physiological stimulation frequencies cause it to recycle continuously with a cycle time in the range of seconds. The RRP is defined to contain synaptic vesicles that immediately fuse upon stimulation by action potentials. This definition of the RRP assumes a homogeneous release probability among all vesicles in the pool. Yet, increasing evidence indicates a degree of heterogeneity among vesicles (see review [35]). The violation of the pool homogeneity assumption may lead to an appreciable difference for pool size and release probability estimations [35]. The RRP constitutes around 5% of the total vesicle pool [25,28]. The time constant of its replenishment at rest is around several seconds (5 to 10 seconds) but is highly modulated by neuronal activity. The RP together with the RRP constitute the total recycling pool. In addition to these three vesicle pools, a small group of vesicles rapidly released by short depolarization is termed the immediate releasable pool (IRP). The IRP is a subset comprising 10–25% of the RRP vesicles in neuroendocrine cells [36,37]. The IRP was proposed to represent RRP vesicles located in close proximity of VGCCs, which are therefore exposed to a higher Ca^{2+} concentration occurring with a shorter time delay than the other vesicles in the RRP. These vesicles are also referred to as superprimed vesicles [38,39].

The individual synapse's efficacy of signal transmission is determined by the vesicle number, pool size and release probability. The functional heterogeneity of signal transmission and synaptic plasticity at different synapses partially reflects the considerable variation of the total vesicle pool size which largely determine the synaptic release probability. In hippocampal autaptic neurons culture, it was reported that stimulation protocol inducing long-term depression causes a parallel decrease in the pool size [40]. In dissociated hippocampal culture, methodology based on FM-styryl dyes, photoconversion and correlative structural methodology found that synaptic strength follows the number of docked vesicles but is not

correlated with the total number of vesicles at a terminal. This is likely due a large fraction of resting vesicles [41]. Using the same methodology at CA3-CA1 hippocampal terminals undergoing long-term potentiation (LTP), the total recycled vesicle pool near the active zone approximately doubles in size [42]. Interestingly, the smallest terminals showed the greatest relative expansion. At the Calyx of Held, induction of post-tetanic potentiation (PTP) by high frequency stimulation (HFS) change the balance between the fast and slowly releasable pool but the sum remains unchanged [43]. To summarize, accumulating investigations confirm that pools might be key substrates changing synaptic efficacy, although it is still unclear how the size of the pool scales with synaptic performance.

The active zone

The active zone is an electron-dense structure associated with the presynaptic plasma membrane, stabilized by a protein scaffold and organized by a cytoskeletal matrix which contains several multi-domain proteins including bassoon, piccolo, RIM, Munc13, Liprins, RIM-BP and ELKS proteins [44]. This complex docks and primes synaptic vesicles for exocytosis, clusters Ca^{2+} channels to the release site and spatially aligns the postsynaptic density (see Figure 1) via trans-synaptic cell-adhesion molecules [12].

Recruitment of synaptic vesicles to the AZ is traditionally accepted to occur in two sequential steps: docking and priming [45,46]. However, the main distinction between the two processes is methodological. The number of docked vesicles is assessed by morphological study, identifying vesicles near or attached to the plasma membrane using electron microscopy [47]. On the other hand, primed vesicles are quantified by a functional measurement of rapidly releasable vesicles [35]. Vesicles can be rapidly recruited to the AZ during sustained stimulations, reloading into the RRP within few milliseconds [48,49]. In the Calyx of Held, few vesicles are docked per AZ, on average ~2 [50], compared to ~5 to 10 in hippocampal neurons [51] and ~5 vesicles are within 20 nm of an active zone [50,52]. After docking to the presynaptic active zone (AZ; see Figure 1) vesicles are not immediately releasable. To become fusion competent, they have to be primed by a Munc13/CAPS-dependent reaction [53] which is accompanied by the assembly of a fusogenic protein complex (detailed in section 1.2). This so-called SNARE ((Soluble NSF Attachment Protein Receptor) complex maintains the fusion competent vesicles in a metastable releasable state until a sufficient trigger reaches the AZ. Action potentials (APs) elicit a large increase in $[Ca^{2+}]_i$ by opening voltage-gated Ca^{2+} channels (VGCCs) clustered at the AZ. The Ca^{2+} ions bind to and activate nearby Ca^{2+} sensor proteins (Figure 2), which rapidly trigger secretion in conjunction with the SNARE complex and its associated proteins. Ca^{2+}-influx is estimated to yield peak intracellular Ca^{2+} concentrations reaching approximately 100 µM within 10 to 45 nm distance from the channel opening [54]. The corresponding Ca^{2+} influx `sphere´ is referred to as a microdomain or nanodomain. Within the microdomain, Ca^{2+} sensors are likely to trigger vesicular fusion (Figure 2), (the likelihood being highest at the center of the microdomain). The microdomain corresponds to the area where superprimed vesicles are located. Superpriming was proposed to be a rapid actin-dependent positional process [39] bringing vesicles closer to Ca^{2+} sources. Alternatively, a mechanism intrinsic to the vesicle fusion machinery may impose a higher Ca^{2+} sensitivity causing fast transmitter release [55].

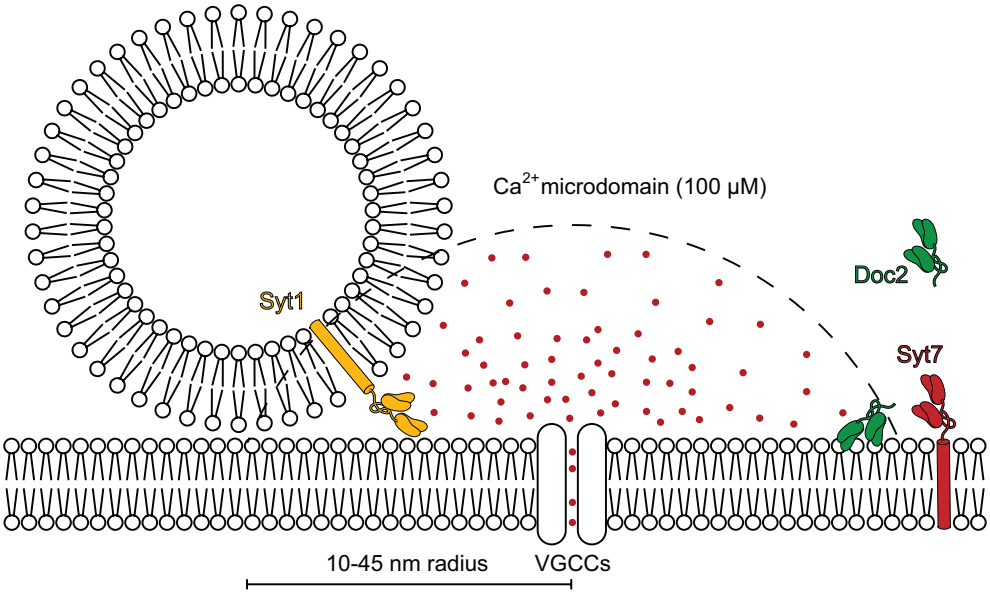

Figure 2. At Ca^{2+} microdomains, the Ca^{2+} channels and Ca^{2+} sensors are in close proximity. Zoom-in on the spatial micro/nanodomain organization of Ca^{2+}-channels with the vesicular release machinery, orchestrating vesicle fusion. Upon depolarization, when a Ca^{2+} channel opens temporarily, vesicles in different locations are exposed to different Ca^{2+} peak concentrations. 'Superprimed' vesicles are either exposed to higher Ca^{2+} concentrations or have an increased Ca^{2+} sensitivity, supporting very fast release [54,64]. Vesicles outside the microdomain will show lower release probabilities and slower kinetics. For diffusible Ca^{2+} sensors, the relatively slow diffusion of proteins may cause even longer delays. Different Ca^{2+} affinities and biophysical properties of the Ca^{2+} sensors as Syt-1 (yellow), Syt-7 (red) and Doc2 (green) add further heterogeneity in Ca^{2+}-secretion coupling.

Synaptic vesicle fusion (through membrane pore formation or full vesicle collapse) discharges the vesicle content in the synaptic cleft. This secretion event is followed by membrane reuptake. A pathway for synaptic vesicle retrieval is mediated by clathrin-coated endocytosis (Figure 1). An alternative cycle exists, referred to as kiss-and-run where the shape and identity of the vesicle is preserved [56,57] and the recycling is potentially much faster which is an advantage for continuous high-frequency information transfer. The existence of an ultrafast mode of endocytosis operating in parallel of coated-vesicles recycling in neurons is now established. Capacitance measurements in endocrine cells [58] and the Calyx of Held [59] strongly supported the concept. Investigations in *C. elegans* neuromuscular junctions [60] and mouse hippocampal neurons also endorse local ultrafast endocytosis and recycling [61]. Whether kiss-and-run constitutes the major mode of local recycling is uncertain (for review [4,62]) and only a fraction of the RRP vesicles might go through this pathway [56,63].

1.2 The core protein machinery for synaptic release

Accurate synchronicity of vesicle fusion with presynaptic APs involves the interplay of a core protein complex essential for Ca^{2+}-dependent secretion, involving the SNARE complex, SNARE-accessory proteins and Ca^{2+} sensor proteins. This machinery is the driving force for membrane fusion in a manner that is both extremely fast and highly Ca^{2+}-dependent.

This section will introduce some, but not all proteins controlling the synaptic release of neurotransmitters.

1.2.1 SNAREs

To bring the vesicle membrane in tight contact with the plasma membrane and engage docking, priming and fusion of vesicles, the formation of the SNARE (Soluble NSF Attachment Protein Receptor) complex is required. The synaptic SNARE complex consists of three proteins: synaptobrevin-2 (also named VAMP2 for Vesicle Associated Membrane Protein 2), syntaxin-1 and SNAP-25 (Synaptosome Associated Protein 25). Synaptobrevin-2 is attached to synaptic vesicles via its C-terminal transmembrane domain (TMD) and is therefore called a v-SNARE. Syntaxin-1 and SNAP-25 are associated with the plasma membrane (PM; the target membrane for secretion) and are therefore called t-SNAREs (Figure 3). Syntaxin-1 is anchored to the PM via its TMD whereas SNAP-25 is PM-associated via cysteine-linked palmitoyl chains. All three proteins contain coiled coil domains, called the SNARE motifs, which strongly bind together to form a four-α-helix bundle [65,66] (for review [67]). SNAP-25 inserts two coiled coil domains (Figure 3). SNARE complex assembly starts at the membrane distal-end of the SNARE domains and proceeds gradually ('zippering') towards the transmembrane domains [68]. The initial state is referred to as the trans-SNARE complex. Complete SNARE zippering finally results in a so-called cis-SNARE complex where the two membranes have fused and the TMDs are aligned [69]. During docking and priming, partial assembly of the SNARE complex already takes place but progression ('zippering') to the fully assembled cis-SNARE complex is blocked in absence of the Ca^{2+} signal [70]. SNARE complex assembly provides much energy required for membrane fusion, which helps to overcome a significant energy barrier caused by dehydration of the phospholipid surface and the reorganization of lipid structures in the membrane [68,71]. It has been suggested that assembly of at least 3 SNARE complexes provides the required energy for fast release [72] but different approaches have delivered divergent estimates about the stoichiometry of the presumed fusion complex (for review [70]).

1.2. 2 Docking and priming by SNARE-accessory proteins

Other proteins that bind to SNAREs are also required for synaptic fusion, including Munc13 and SM-proteins [73]. Munc18 (Mammalian uncoordinated-18) proteins are the mammalian homologues of UNC-18 which was first discovered in *C. elegans* [74] where its mutation induced an accumulation of cholinergic vesicles and a paralytic phenotype [75]. The mouse ortholog Munc18 was characterized to be essential for SNARE-mediated membrane fusion [76] (for review [69]) and is a key contributor of synaptic release in mouse neocortical neurons [76]. Munc18-1 protein is enriched in neurons and synapses and is essential for both vesicle docking and priming [77]. It regulates the association of the SNARE complex by binding the N-terminal of syntaxin [78] which promotes its stability and to the C-terminal SNARE motif of synaptobrevin [79]. Munc18-1 first bind to the self-inhibited "closed" conformation of syntaxin-1 [80,81] and later to synaptobrevin to template SNARE complex assembly [81]. Munc18 also physically interacts with the vesicle associated protein Doc2 [82]. The functional relevance of the Munc18/Doc2 interaction has not yet been elucidated.

Sec1 was first identified as an essential factor for exocytosis in *Saccharomyces cerevisiae* where a defective Sec1-1 mutant caused the accumulation of intracellular membrane bound vesicles [83]. Later, a mammalian ortholog n-Secl was characterized [84] and isolated in rat neural-specific tissues as a syntaxin-binding partner, which participated in the regulation of synaptic vesicle docking and fusion [85]. The proteins shows a high degree of evolutionary conservation, forming the conserved Sec-1/Munc-18 (SM) protein family.

Another SNARE-binding protein Munc13 was identified as mammalian homolog of UNC13, a gene implicated in movement coordination in *C. elegans* [74]. In mice, neurons lacking Munc13-1 suffer from a limited Ca^{2+}-dependent neurotransmitter release [86]. The SNARE motif of syntaxin-1 is initially shielded by its autonomously folded Habc domain, a three-helix bundle [87] which makes the SNARE motif inaccessible for association with synaptobrevin-2 and SNAP-25 [88]. The MUN domain of Munc13-1 catalyzes the transition from the Munc18-1/Syx1 complex to the SNARE complex in the presence of SNAP-25 and synaptobrevin-2 [89–92]. An illustrative example of Munc13 function was provided by the LE mutant of Syntaxin-1A which bypasses the requirement of Munc13-1 in adopting a constitutive open conformation and partially restore evoked neurotransmission and locomotion [93]. Two conserved residues (R151, I155) were identified in syntaxin-1 linker region, essential for MUN domain association while still bound to Munc18 [91]. This binding initiates a conformational change in syntaxin to allow ternary complex formation. Yet, the MUN domain does not dissociate the closed Munc18-1/syntaxin-1 complex [91,94]. RIAA mutations (R151A and I155A) induced a loss of liposome fusion [91]. In neurons, the same mutations impair spontaneous, evoked neurotransmission and sucrose-induced release [91]. Independent *in vitro* FRET and single-vesicle fusion assays confirmed the crucial Munc13-1/Munc18-1 collaboration which ensures proper SNARE complex assembly [95]. In the current working model, Munc18-1 initiates SNARE complex assembly while Munc13-1 bridges the vesicle and plasma membranes [96] and helps opening syntaxin-1 [90]. Finally, both Munc18 and Munc13 are essential for SNARE-dependent fusion as they also prevent premature disassembly of the SNARE complex by NSF [97]. Munc13 might provide additional means to regulate membrane fusion as its C_1 domain binds DAG, at least some of its C_2 domains bind phosphatidylinositol (4,5)-biphosphate (PIP_2)/$Ca^{2+}$and further Ca^{2+} sensitivity is encoded in a calmodulin-binding motif [98].

Complexin is another essential component for the final Ca^{2+} triggering step [99] especially for the fast release component [100]. It is thought to associate with the SNARE bundle between syntaxin and synaptobrevin [101] in order to stabilize the syntaxin/synaptobrevin interface. Complexin promotes a metastable state of SNARE complexes and simultaneously blocks fusion, thereby rendering the vesicles in a primed state [102]. This is critical for synchronization of release during the short time window of Ca^{2+} rise [100].

Several other synaptic proteins may regulate the assembly of SNARE complexes. Tomosyn [103] and amisyn [104] have a C-terminal R-SNARE motif that can substitute for synaptobrevin in the synaptic SNARE complex and inhibit premature exocytosis by interfering with synaptobrevin association into the SNARE complex.

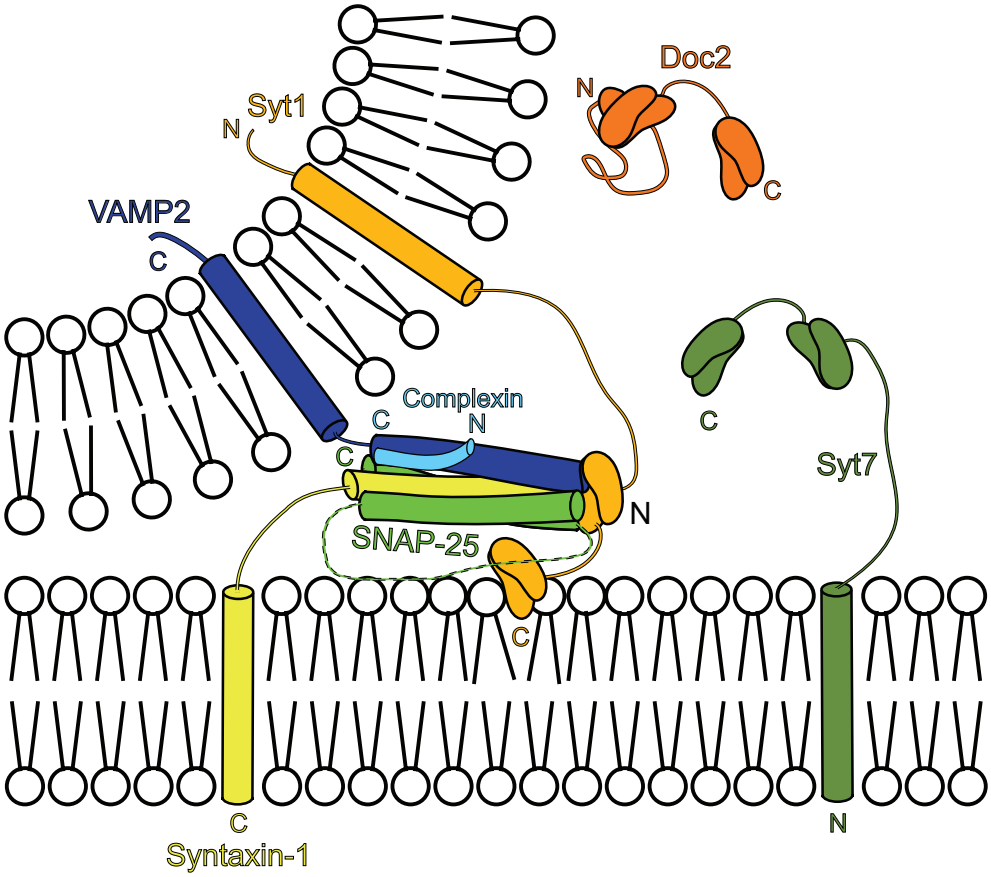

Figure 3. Model of SNARE-complexin-Ca^{2+} sensor complex. Cartoon representation of the SNARE complex in trans-conformation formed by Syntaxin-1 (light yellow), VAMP2 (dark blue) and SNAP-25 (light green) together with complexin (light blue) and Ca^{2+} sensors, Synaptotagmin-1 (light orange), Synaptotagmin-7 (dark green) or Doc2b (dark orange). The coiled coil SNARE motifs zipper together from N- to C-terminal, together forming a four-α-helix bundle docking the vesicle to the plasma membrane. Ca^{2+} sensors and complexin associate to the SNARE-membrane interface and form a Ca^{2+}-sensitive clamp of membrane fusion. It is not yet clear if Syt-1, Syt-7 and Doc2 directly compete or complement each other in response to different types of Ca^{2+} signals.

1.2.3 Vesicle fusion regulators: Ca^{2+} sensors

1.2.3.1 C_2 domain proteins

In addition to the SNARE complex and its accessory proteins, vesicle fusion requires Ca^{2+} sensor proteins for the process to be Ca^{2+}-sensitive. Various Ca^{2+} sensors modulate presynaptic strength and release kinetics. Most contain multiple C_2-domains [105,106]: conserved protein motifs comprising approximately 130 amino acids initially identified as a conserved domain of protein kinase C (PKC) [107]. From the Pfam database, C_2 domains are predicted in 127 human proteins [108], making the C_2 domain one of the most abundant lipid-binding domains in eukaryotes.

Single C_2 domains usually function as a Ca^{2+}-dependent membrane binding module (e.g. to direct enzymatic activity to a specific site at the membrane) [106]. Structurally, a C_2 domain is made of eight β-strands forming a barrel-like structure. Five negatively charged amino-acids (typically aspartate or less frequently glutamate) cooperate to bind 2 to 4 Ca^{2+} ions, thus forming a Ca^{2+} binding pocket (CBP). Ca^{2+}-binding reverses the net negative charge present on C_2 domain surface, enabling interactions with negatively charged phospholipid head groups and the insertion of surrounding loops into the hydrophobic phase of membrane bilayers [109].

Typically, neuronal Ca^{2+} sensors contain two C_2 domains in tandem, called C_2A and C_2B, which bind Ca^{2+} and phospholipids. The precise mechanism of membrane fusion trigger may result from allowing SNARE complex zippering to proceed, as well as membrane dynamics. The insertion of wedge-shaped structures induces bending and lipid reordering, lowering the energy barrier and enhancing the probability of membrane fusion [110]. This process requires at least two C_2 domains as a single C_2 unit cannot induce membrane curvature [111].

1.2.3.2 Synaptotagmins

The main Ca^{2+} sensor family is formed by the Synaptotagmins (Syts), composed of an N-terminal transmembrane domain, two C_2 domains C_2A and C_2B, connected together by a linker which varies in length between isoforms [114]. Different Syts display distinct expression patterns, subcellular localizations and biochemical properties. Of the 17 isoforms identified, eight (Syt-1, 2, 3, 5, 6, 7, 9 and 10) bind Ca^{2+} and regulate vesicle fusion [115]. Syt-1, Syt-2 and Syt-9 operate as fast release sensors for synchronous release [116]. Most neurons express either Syt-1 or Syt-2 [117], considered to be the main Ca^{2+} sensors for triggering synchronous neurotransmitter release in response to APs [116,118–121]. Syt-1 is a vesicle-bound protein via its TMD. It contains two Ca^{2+} sensing C_2 domains, C_2A and C_2B with three and two Ca^{2+} binding sites respectively [122–124]. Syt-1 was shown to link membranes [125] and SNAREs [126], inhibiting spontaneous fusogenic activity of the release machinery [127]. After Ca^{2+} binding, this inhibition is released, while fusion is promoted by inducing lipid bilayer bending [128,129].

Upon SYT1 ablation, synchronous neurotransmitter release is impaired, desynchronized but not completely abolished in Syt1-expressing neurons. Syt-2 and Syt-9 can compensate for Syt-1 loss [116]. Syt-7, which shows different membrane interaction kinet-ics of its cytoplasmic domains and is also differently localized at the PM, drives the remaining asynchronous component of AP-evoked release [117,130–133]. It contributes to short-term plasticity [133,134], synchronous release fidelity [130] and Ca^{2+} dependent RRP replenishment [135].

For Syts to function properly, it requires Complexin, an important modulator of the release machinery. Complexin also interacts directly with Syt-1 [126,136] which together with the SNARE complex, composes a Ca^{2+}-dependent substrate for primed vesicles which inhibits spontaneous fusion at rest and synchronizes fusion upon AP-dependent Ca^{2+}-influx [100,126,137].

1.2.3.3 Doc2

Spontaneous release is promoted by the double C_2 domain proteins Doc2a & b [133,138,139]. Doc2 proteins share structural and functional properties with Syts. Doc2 also presents a CBP in each C_2 domain. Crystallography and $^{45}Ca^{2+}$-binding assay methods evaluated the affinity and stoichiometry of Ca^{2+} binding to isolated Doc2b C_2 domains and concluded that both C_2A and C_2B bind two Ca^{2+} ions each [140]. Both C_2B and C_2AB display a nearly identical affinity for Ca^{2+} (Kd of 9.6 ± 0.1 and 9.84 ± 0.3 µM respectively) [140]. In the same study, Ca^{2+}-binding to C_2A could not be detected below [Ca^{2+}]free ~100 µM. This observation was confirmed by ITC (Isothermal Titration Calorimetry) [141]. These results suggest that in absence of lipids within the tandem C_2AB, the C_2A domain does not contribute much to the whole protein Ca^{2+}-binding properties. Yet, C_2A exhibits a robust Ca^{2+}-dependent lipid binding [141]. In presence of lipids, membrane translocation occurs with a higher apparent Ca^{2+} affinity, reflected by a lower EC_{50} value of ~1 µM, ~0.5 µM, ~0.24 µM and ~ 0.35 µM respectively for C_2A, C_2B, C_2AB and full length protein [140,142]. Therefore, the apparent affinity for Ca^{2+} strongly depends on the presence of negatively charged lipids and is an absolute requirement for C_2A activity. Membrane translocation monitoring in chromaffin cells reported much higher affinities for Doc2a and -b translocation (Ca^{2+} EC_{50} concentrations of respectively 450 nM and 175 nM) [140,143] than for Syts (~10 to 20 µM for Syt-1/2 and 1-2 µM for Syt-7) [144]. Both Doc2s and Syts contain a lysine rich sequence within the C_2B domain, called polybasic stretch which binds to SNARE proteins and also the phospholipid PIP_2 [145–147].

Doc2 differs from Syts by the absence of a TMD in the N-terminal region. In addition to spontaneous release, Doc2 has also been implicated in asynchronous release [141,148,149] but this function is still under debate [150,151].

1.2.3.4 Interplay of multiple Ca^{2+} sensors in secretion

Complex stimulus-responsiveness of synaptic secretion can originate from different vesicular release probabilities (P_{vr}) in response to various calcium dynamics in the pre-synaptic terminal [29,115,152,153]. The origin, function and interplay between the different types of release seems mostly based on the activity of Ca^{2+} sensors but the underlying mechanism remains unclear and debated. Given the redundancy and co-expression at the cellular level of Ca^{2+}-sensing proteins involved in secretion [117], it is likely that they act in concert upon Ca^{2+} elevation [152].

Electrophysiology studies revealed that genetic inactivation of fast Ca^{2+} sensors not only abrogates the fast neurotransmission, but also alters the Ca^{2+} cooperativity of asynchronous and spontaneous release. Upon Syt-1 & -2 elimination, asynchronous release becomes apparent and spontaneous frequency increases approximately tenfold [23,120,159,133,138,139,154–158]. Yet, in the presence of Syt-1/-2, genetic inactivation of Syt7 only mildly affect short-term plasticity [130,134,160]. Also, in presence of Syt-1, DOC2 ablation does not alter spontaneous release [133,161]. One interpretation is that other Ca^{2+} sensors are unclamped in the absence of fast Syts.

A dual or multiple Ca^{2+} sensor model considers that different release kinetics may originate from the competition for the same pool of vesicles by multiple Ca^{2+} sensors presenting different biophysical properties. This concept combines two distinct hypotheses that one can term 'clamping by site occupancy' and 'release of inhibition'. The first theory considers that Ca^{2+} sensors promote fusion. The inhibition would then be mediated by competition of sensors for the same release site (occupancy). A supportive observation is the competitive association of Syt-1 and Doc2b with SNARE proteins syntaxin-1 and SNAP-25 in a Ca^{2+}-independent manner [138]. Hypothetically, genetic inactivation of fast SYTs would vacate SNARE complex binding sites, becoming available for Syt-7 and Doc2s. The alternative explanation takes into account that fast Ca^{2+} sensors inhibit premature fusion until Ca^{2+} influx. This mechanism relies on the association of Syt-1/2 with complexins and SNAREs [126,137,162,163]. In addition, variation in the proximity between a Ca^{2+} sensor and the Ca^{2+} source (see Figure 2) can affect the kinetics of neurotransmitter release kinetic.

In summary, the redundancy and diversity of Ca^{2+} sensors, each with potentially distinct synaptic distributions and different SNARE, Ca^{2+}, and membrane binding properties, are fundamental determinants of neurotransmission. Hence, a better understanding of the interplay between those sensors is needed to fully understand how they modulate neurotransmitter release.

Box 1: The distinct phases of neurotransmitter release

Neurotransmitter release is separated in three distinct phases with different kinetics and triggering mechanisms (Figure 4) which are dependent on distinct Ca^{2+} sensors. During stimulation by a single or repetitive AP, phasic (synchronous) release represents most of the postsynaptic current. Synchronous neurotransmission is tightly linked to stimulation and appears on average within 60 microseconds after the upstroke of the presynaptic action potential which allows massive Ca^{2+} entry into the presynapse [112]. When a nerve terminal is stimulated repeatedly at a high rate, the postsynaptic current amplitude drops dramatically and eventually reaches a lower steady-state level (Figure 4). Under these conditions when the fast rising currents from synchronous release become very small, the steady state current primarily originates from a slower process, named asynchronous or tonic release. This component is not clearly identifiable in the postsynaptic response from a single stimulation, because this minor component is mixed together with the synchronous phase. During repetitive stimulation however, the asynchronous phase builds up to a major component (Figure 4) which is attributed to residual Ca^{2+} accumulation in the synaptic cytoplasm. The build-up of asynchronous component in parallel to synchronous component rundown (Figure 4) can be explained by their strive for the same fusion competent vesicle pool. Finally, a third form of neurotransmitter release occurs stochastically in absence of APs. This phase is termed spontaneous release [113] (Figure 4).

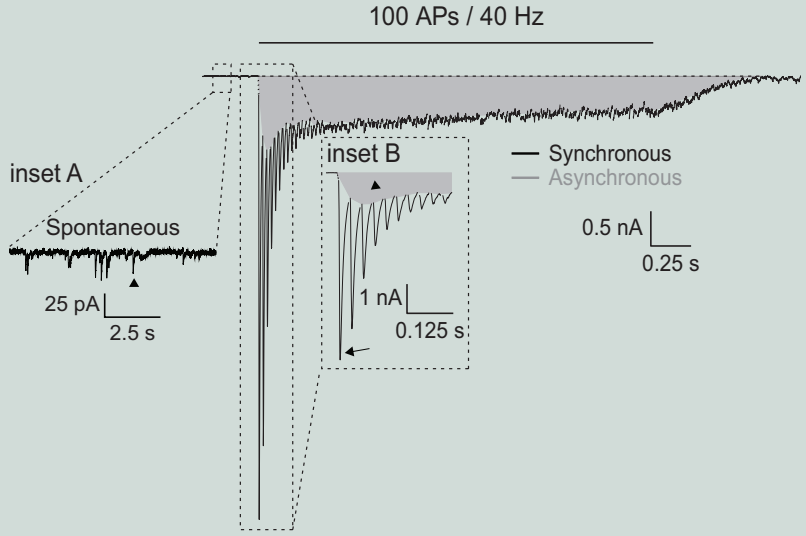

Figure 4. Three different types of neurotransmitter release kinetics. Representative scheme showing whole-cell electrophysiology recordings of postsynaptic current from a wild type excitatory hippocampal neuron in primary culture. The naive cell was recorded first in resting condition (left, inset A) and then during a high frequency stimulation at 40 Hz (right, inset B). Recordings at rest show spontaneous glutamate release. These events are also termed mEPSCs or minis (arrowhead in inset A). The train stimulation enables to identify phasic (synchronous, arrow in B) and tonic release (asynchronous, arrowhead in B), together constituting the total evoked release. Although all phases contribute to the measured postsynaptic current, the synchronous and asynchronous current charge can be approximated by calculating the white and grey area in the current plot, respectively (best visible in inset B).

2. Vesicular fusion and membrane composition

Membrane interactions play an important role in C_2 domain protein activity and membrane fusion. Vesicle cycling is orchestrated by proteins, lipids and their interactions. Membrane trafficking and fusion depends on local lipid composition within clusters, known as lipid rafts [164,165]. They influence synaptic signal transduction and represent part of the mechanism modulating neurotransmission (for review [166]). The next section introduces several important membrane components that are known to affect Ca^{2+}-dependent membrane fusion in conjunction with the protein machinery.

2.1 Phospholipids

Synaptosomal membranes contain three major types of lipids: phospholipids, cholesterols and sphingolipids [167]. The main phospholipids present in neurons membrane and trafficking vesicles are phosphatidylcholine (PC), phosphatidylethanolamine (PE), phosphatidylserine (PS) and phosphatidylinositol (PI) [16,168,169]. They can be classified by the electric charges they carry. PE and PC are neutral. Those phospholipids are not directly involved in the membrane association of Syt-1 and Doc2, yet they are believed to induce membrane curvature stress [170] and to be involved in fusion in collaboration with C_2 domain proteins [171]. PI is a minor component located on the cytosolic leaflet of the cell membrane which carries one negative charge through its phosphate group. It is converted by phosphorylation to PIP_2 which can subsequently be hydrolyzed into DAG and IP_3 by phospholipase C.

2.1.1 Phosphatidylserine

Phosphatidylserine (PS) is the major acidic phospholipid class present in cell membrane. It accounts for 13-15% of the phospholipids in the human cortex [172] and carries a single negative charge. PS is exclusively localized in the inner leaflet of membrane except during apoptosis where its externalization serves as a phagocytosis signal [173]. It forms part of protein docking sites and is necessary for several signaling pathways including PKC signaling and exocytosis [174,175]. It is involved in Ca^{2+} dependent membrane association of many C_2 domains, including those of Synaptotagmin-1 and Doc2a/b and increases their apparent affinity for Ca^{2+} [176–178].

2.1.2 Phosphatidylinositol (4,5)-biphosphate (PIP_2)

Phosphatidylinositol (4,5)-biphosphate (PIP_2) is an essential phospholipid present in small amounts in the inner leaflet of the PM. It is locally synthesized by the phosphorylation of phosphatidylinositol (PI) catalyzed by the sequential activity of PI-4-kinase, yielding PI(4)P and PI(4)P-5 kinase. $PI(4,5)P_2$ forms clusters at exocytic domains [166]. It contributes to the regulation of transporters and channels [179], exocytosis [146,180,181] and endocytosis [182]. The molecular function of PIP_2 depends on its highly negative headgroup which enables C_2 protein anchoring to membranes. Some synaptic proteins, typically containing polybasic peptide sequences are targeted to clusters enriched in presynaptic phosphatidylinositides (PI, PIP_2 and PIP_3) [181,183] where anionic lipids modulate their Ca^{2+}-sensitivity and induce their activation to enhance membrane fusion [184–186]. Depletion of PIP_2 and/or PIP_3 from the PM does not affect PKC association to the PM but accelerates its dissociation [185]. Both Syt1 and Doc2b show Ca^{2+}-independent membrane penetration in membranes containing PIP_2 [138,183,184,187].

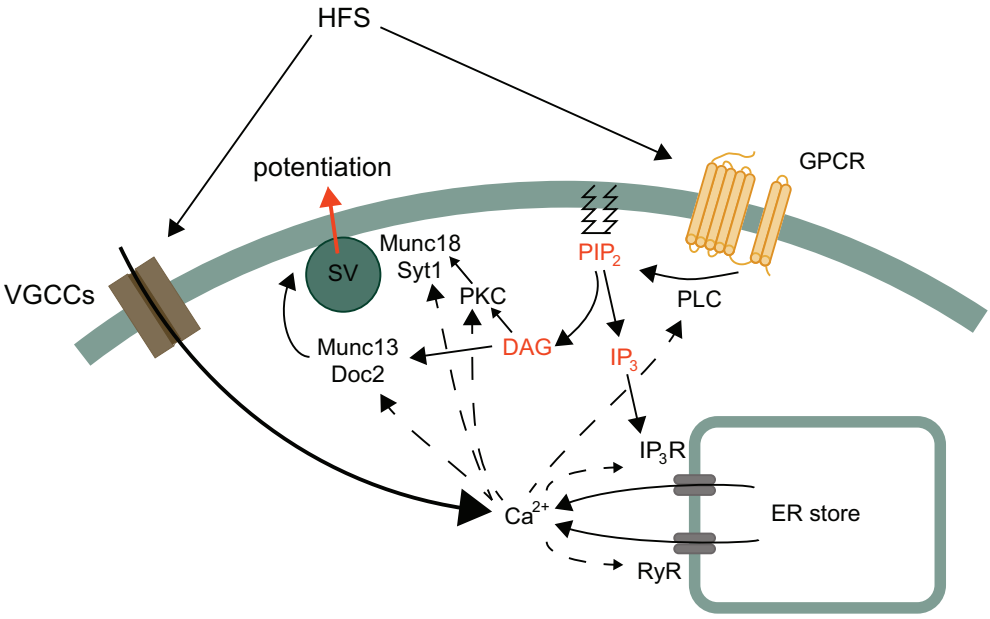

Figure 5: DAG/PLC potentiation pathway in relation to Ca^{2+}-triggered secretion. Overview of the presynaptic DAG potentiation pathway originating from PIP_2 hydrolysis into IP_3 and DAG (diacylglycerol) following high frequency stimulation (HFS) or G-protein activation. Bulk Ca^{2+} accumulation during tetanic activity leads to DAG production. DAG activates C_1 domains in both Munc13 and PKC, while Ca^{2+} can bind to C_2 domain proteins (Syts, Doc2s). PKC phosphorylates Munc18, which also causes potentiation. Adapted from [190,201–205].

Their association with PIP_2 is dependent on the polylysine basic charges on the C_2B domain surface which also interacts with the SNARE complex [188]. PIP_2 interaction is crucial for Doc2b targeting to the plasma membrane together with Ca^{2+}. Reduction of PIP_2 levels by rapamycin which depletes PIP_2 without altering Ca^{2+}, DAG or IP_3 [189],abolishes Doc2b translocation [183]. PIP_2 interaction with C_2 domain proteins facilitates the close apposition of the vesicle to target membrane [146,187], promotes exocytosis and induces synaptic potentiation [190]. PIP_2 is hydrolyzed into IP_3 and DAG by phospholipase C (PLC) (Figure 5). Those 2nd messengers are also crucial for Ca^{2+}-dependent potentiation of exocytosis (Figure 5) [166].

2.1.2 Cholesterol

Cholesterol is an abundant sterol in synaptosomes [167]. In contrast to phospholipids, cholesterol diffuses rapidly between the two membrane leaflets. It is a critical regulator of exocytosis by distinct mechanisms. First, it modulates the biophysical properties of the membrane by reducing membrane fluidity. The enhanced membrane rigidity by cholesterol adds resistance to the membrane which influences fusion pore dynamics [191,192], vesicle motion and docking [193] and the kinetics of vesicular release [194]. Second, cholesterol is required for the clustering of syntaxin 1 and SNAP-25 on the plasma membrane [195,196] and their redistribution was observed upon depletion of cholesterol from the plasma membrane [195,197,198]. Cholesterol depletion results in inhibition of secretion in neuroendocrine cells [195,196].

In hippocampal cultures, cholesterol depletion leads to an augmentation of spontaneous neurotransmission and severe impairment of the evoked component [199,200].

2.2 Lipid dynamics from stalk formation to pore expansion

The fusion of synaptic vesicles with the plasma membrane requires complex rearrangements of the two phospholipid bilayers. This complex reaction involves several intermediate steps. The first is the contact between the vesicular and plasma membrane phospholipid bilayers. The two membranes are bent towards each other forming local curvatures termed protrusions. The fusion process then continues, forming a stalk where the outer synaptic vesicle leaflet and inner plasma membrane layer become continuous and create a bridge [69]. Lipid rearrangement on both sides proceeds further after the stalk formation, resulting in bilayer formation between the luminal vesicular leaflet and the outer membrane leaflet. From this hemifusion state, tension induces a breach into the single bilayer, creating a fusion pore [206]. The fusion pore is stabilized and expanded to enable neurotransmitter release into the synaptic cleft. Those steps require substantial energy to overcome membrane repulsion. This energy is provided by the SNAREs and Ca^{2+} sensor proteins. C_2 domain proteins such as Syts and Doc2 enhance the formation of highly curved membrane tubules from liposomes, are associated with elongated membrane structures that tether opposing membrane bilayers and enhance the probability of membrane hemifusion in cell-free preparations [207,208].

Box 2:

In vitro methods to study phospholipid- and Ca^{2+}- binding by C_2 domains.

Phospholipid binding assays.

To measure phospholipid binding by isolated C_2 domains, a phospholipid aggregation assay can be used [209]. In this assay, lipids are dissolved and mixed in an organic solvent (e.g. chloroform) and dried under argon or nitrogen flow to prevent oxidation. After adding an aqueous solution, the lipids form vesicles of various sizes (large and small, multilamellar and unilamellar structures). Sonication is used to break these vesicles into small unilamellar vesicles (liposomes) that can be used in various assays. To assess protein-lipid binding, an aggregation assay is performed. It consists of a kinetic measurement of the optical density of a solution at a wavelength of 350 nm. The solution contains liposomes made with a PC/PS lipid mixture and a calibrated $[Ca^{2+}]$ free solution. After a baseline recording, C_2 domain protein fragments are added, which induce a rapid aggregation of the liposomes, increasing the absorbance depending on $[Ca^{2+}]$free and the Ca^{2+} affinity of the protein fragment. After testing various $[Ca^{2+}]_{free}$ solutions, the Ca^{2+} concentration that induces half-maximal liposome aggregation as a measure for the Ca^{2+} affinity of the protein fragment. The dose-dependent activity usually resembles a Hill curve, caused by the fact that Ca^{2+} ions bind to C_2 domains in a cooperative manner. The Hill coefficient gives an estimate of the number of Ca^{2+} ions cooperatively binding each Ca^{2+}-binding-pocket.

Another common method is the pulldown assay. In this assay, a buffered $[Ca^{2+}]_{free}$ solution is directly mixed together with liposomes and recombinant C_2 proteins. After incubation, the solution is subjected to high speed centrifugation to separate the liposomes (which form a pellet) and the supernatant. The amount of protein in each fraction is then determined by SDS-PAGE or Western-blot. The quantity of protein found in the pellet indicates its capacity to bind lipids. The procedure is repeated in a range of $[Ca^{2+}]_{free}$ to determine the Ca^{2+} affinity.

Optical tweezers [208] or pull force measurements is a recent technique which allow fine manipulation of vesicles. It requires lipid bilayers formed on the surface of polystyrene beads. Vesicles are optically trapped by a focused laser beam. A bead position detector registers the bead displacement from the optical trap, which allows to measure force exerted onto the bead. This enables the measurement of the force with which two beads become tethered. An advantage of this assay is the ability to control phospholipid composition and to measure unitary membrane fusion events. The main limitation of this assay resides in the fact that membrane dynamics and deformation cannot be completely identical to the physiological state, such as in living cells where SNAREs, accessory proteins and additional factors are all present (in other words: living systems are more complete but less defined).

Ca^{2+} binding assay

For the direct measurement of Ca^{2+} ions binding to C_2 domain proteins recombinant C_2AB domains can be incubated with radioactive $^{45}Ca^{2+}$ ions, binding of which can be

quantitated after ultrafiltration procedure and measurement of the protein sample compared to filtrate radioactivity [140,210].

An alternative to the use of Ca^{2+} isotopes is isothermal titration calorimetry [141,211]. This method measures the heat consumed or released in an endothermic or exothermic reaction. In this case Ca^{2+} binds to aspartate residues within C_2 domains inducing a change in the entropy (S).

Other methods to detect Ca^{2+} binding are NMR spectroscopy [124,212] or spectrofluorometry of aromatic amino acid residues [133,212]. The latter method has been used to measure Ca^{2+} binding for Syt-1 and Doc2b and makes use of the changes in fluorescence from aromatic residues in the surrounding of Ca^{2+} binding sites upon Ca^{2+} binding [133].

3. Ca^{2+} sources for exocytosis

Close proximity of Ca^{2+} sensors to Ca^{2+}-channels optimizes the efficiency of Ca^{2+} sensor activation for fast neurotransmitter release [213,214]. At rest, neurons maintain a low intracellular Ca^{2+} concentration ($[Ca^{2+}]_i$) in the 50-100 nM range [215–218]. In the calyx of Held synapse, which is well accessible to fluorescence-based measurements of presynaptic Ca^{2+}, the Ca^{2+}-dependence of release extends over a wide range from 50 nM to 50 µM [219–221]. At the resting $[Ca^{2+}]$, vesicle release exhibits a low Ca^{2+}-cooperativity. However, above 3 µM Ca^{2+}, the Ca^{2+}-cooperativity for vesicle fusion is around 4 [221]. This may suggest that different ranges of Ca^{2+} concentrations are governed by different sensor proteins which differ in the number of Ca^{2+} ions binding cooperatively to their C_2 domains.

3.1 AP-dependent exocytosis: VGCCs

Voltage-gated calcium channels (VGCCs or CaVs) are the primary mediators of depolarization-induced calcium entry into neurons from the extracellular space [222,223]. Opening of VGCCs results in Ca^{2+} influx along the concentration gradient. Upon depolarization, it was estimated from Ca^{2+}-current measurements that around 30 channels at the Calyx of Held to 40 channels at hippocampal CA3-CA1 synapses per release site open during a single AP [50,224]. VGCC opening/closing kinetics are prompt, resulting in Ca^{2+} transients that last between 400 to 500 µsec, after which Ca^{2+} is immediately buffered effectively and diffuses rapidly in the intracellular space [225]. The Ca^{2+} influx is initially local, restrained to presynaptic nano/microdomains and will subsequently diffuse to form residual Ca^{2+} [224]. At this stage, it may activate different target proteins such as asynchronous Ca^{2+} sensors. The term global $[Ca^{2+}]$ is typically used to refer to the spatially homogeneous $[Ca^{2+}]_i$, after the peak Ca^{2+} signal has diffused. The high diversity of Ca^{2+}-channels fulfill specialized functions depending on neuronal subtype. In most synapses, release is triggered by Ca^{2+} influx through P/Q- ($CaV_{2.1}$) and N-type Ca^{2+} channels ($CaV_{2.2}$) [224,226–231] which are associated with SNARE proteins [232] and Ca^{2+} sensors [233]. The R- ($CaV_{2.3}$) and L-subtypes (CaV_1 series) are involved only rarely [226,227]. Finally, the T-type (CaV_3) Ca^{2+}-channel is important for repetitive firing of action potentials in rhythmically firing cells such thalamic neurons (for review [5,234]).

3.1.1 CICR: Intracellular amplification of evoked Ca^{2+}-transients

A mechanism that potentiates evoked postsynaptic currents is the Ca^{2+}-induced Ca^{2+} release (CICR) mechanism, which amplifies the intracellular Ca^{2+} signal triggered by VGCC opening. The inflow of Ca^{2+} through VGCCs activates IP_3 production from PIP_2 (via metabotropic receptors and PLC). Inositol triphosphate receptors (IP_3Rs) and ryanodine receptors (RyRs) are ligand-activated ion channels located on intracellular membranes. IP_3 binding to IP_3Rs liberates Ca^{2+} from intracellular Ca^{2+} stores. Both the type-I IP_3R [235] and the RyRs [235] are also sensitive to Ca^{2+}, resulting in a direct amplification by the Ca^{2+}-inflow through internal stores. This process of CICR thus propagates Ca^{2+} waves leading to amplification of Ca^{2+} signal [214,236] and inducing short-lasting potentiation [237,238] (for review [239]) but this last point was disputed for excitatory synapses [240] .

3.2 Ca^{2+} sources for AP-independent exocytosis

Despite the low resting $[Ca^{2+}]_i$ at rest, spontaneous release persists in the absence of AP stimulation and under AP blockade by Tetrodotoxin (TTX) [138,237,241–243]. Nevertheless, the rate of spontaneous release remains largely Ca^{2+}-dependent [241,244–246]. To explain this Ca^{2+} dependence, one possible triggering mechanism could be provided by stochastic local Ca^{2+} events which appear randomly in absence of AP (and presence of TTX) [238,241,243]. Several possibilities may lead to such Ca^{2+} signals, involving distinct pathways and different Ca^{2+} sources. First, the activation of PLC via metabotropic receptors can induce intracellular Ca^{2+} fluctuations. Second, the release of Ca^{2+} ions from intracellular stores has been shown to induce spontaneous local Ca^{2+} fluctuations [244,247]. Third, VGCCs which are normally closed during the resting membrane potential may open occasionally with a low probability, giving rise to a Ca^{2+} signal, locally large enough to trigger membrane fusion. Finally, Na^+ channels could spontaneously open when TTX is not present, producing local depolarization, concomitant VGCC activation and Ca^{2+}-influx. These possibilities are further explained in the next sections.

3.2.1 Intracellular source for Ca^{2+} transients
Activation of metabotropic receptors

Another Ca^{2+}-signaling pathway triggering spontaneous release relies on both extracellular Ca^{2+} stimulation and intracellular Ca^{2+}-storage through the activation of metabotropic receptors.

G-protein-coupled receptors (GPCRs) are the largest and most diverse cell surface receptor and hundreds are expressed in the brain [248]. They are activated by different agonists and transduce extracellular signals into intracellular responses via their coupling to G-proteins. The canonical pathway induces intracellular Ca^{2+} oscillations via IP_3 hydrolysis (Figure 5). For example, Gq and Gi induce intracellular Ca^{2+} increase through PLCβ2 and PLCβ1 [249] (see review [222,250]). In general, Gβγ enhances PLC-mediated production of intracellular IP_3. In pyramidal neurons, localized Ca^{2+} transients were mediated by GPCRs activated by glutamate, group I mGluRs (mGluR1 and mGluR5) [251] (for review [252]). The increase of presynaptic Ca^{2+} events through these pathways may lead to an increased spontaneous release rate.

Another example is the Ca^{2+}-sensing receptor (CaSR), a GPCR that can be triggered by $[Ca^{2+}]e$ during moderate synaptic stimulation and induces the enhancement of spontaneous neurotransmitter release through the IP_3R pathway [251,253]. It controls the frequency of Ca^{2+}-transient via the activation of PLC and the subsequent production of IP_3 [251,253].

Stochastic Ca^{2+}-sparks

Early morphological evidence demonstrated by confocal and electron microscopy that the smooth endoplasmic reticulum (SER) constitutes a tubular shaped network, physically continuous throughout neurons [254,255] and locally within axons [256,257]. The ER constitutes a connected intracellular Ca^{2+} reservoir which regulates neuronal Ca^{2+}-homeostasis (see review [258]). Electron microscopy and reconstruction studies of hippocampal synapses [259–261] and other structures [262] (see review [263]) showed the presence of ER closely associated with the presynaptic terminals. Evidence indicates that ER Ca^{2+} signaling in the proximity of release sites modulates spontaneous synaptic transmission.

RyRs and IP_3Rs present on the sarco- and endoplasmic reticulum are responsible for spontaneous Ca^{2+}-transients termed sparks, puffs, syntillas or simply 'transients',. They were observed in hippocampal neurons [237,243] dorsal root neurons [247,264] and cerebellar Purkinje cells [238]. In hypothalamic neurons Ca^{2+} "syntillas" appears in presynaptic terminals in the absence of APs and extracellular Ca^{2+} by a RyR-dependent mechanism [246]. They are likely the same type of spontaneous Ca^{2+} events and will be referred to in this thesis as Ca^{2+}-transients. Ca^{2+}-transients relying on intracellular stores are likely to rise $[Ca^{2+}]_i$ to supermicromolar concentrations over hundreds or nanometers [246]. All IP_3R channels [265,266] and RyRs have a large conductance for cations including Ca^{2+} [267–269] (single channel conductance ranging around 100 pS and ~150 pS for IP_3Rs and RyRs respectively). IP_3Rs were shown to assemble in clusters of similar size which generate the Ca^{2+} puffs [270]. Additionally, clusters can also be formed by a combination of both IP_3Rs and RyRs [271,272]. Ca^{2+}-transients are then likely formed by mixed activation of both receptor types, initiated by few or single receptor clusters opening boosted by the CICR mechanism as released by one of them ignites the activity of its neighbours.

The emergence of Ca^{2+}-transients via IP_3Rs/RyRs remains elusive and the signal that activates the process has not been identified yet. We still need to elucidate whether the mechanism is elicited by stochastic RyR/IP_3R opening, signaling cascade activation following GPCRs and PIP_2 hydrolysis or other Ca^{2+}-dependent activation pathways. In addition, further investigation is necessary to determine if a single receptor opening is sufficient to generate Ca^{2+} transients or not.

3.2.2 Extracellular source for Ca^{2+} transients

VGCCs

Spontaneous Ca^{2+}-transients might originate from the stochastic opening of voltage-dependent Ca^{2+} and Na^+ channels at resting membrane potential. The contribution of VGCCs to stochastic Ca^{2+}-transient generation was mostly investigated through electrophysiological and pharmacological investigations of spontaneous neurotransmitter release, rather than

through direct Ca^{2+}-imaging. A pharmacological blockade of VGCCs in presence of the Na^{+} channel blocker (TTX) revealed that P/Q-, N- and R-type VGCCs contribute to about 50% of AP-independent excitatory minis in hippocampal neurons [241]. T-type channels, also known as low voltage activated (LVA) Ca^{2+}-channels, could also contribute to spontaneous Ca^{2+}-transients because they can be activated at resting membrane potential [234,273]. Also, L-type VGCCs ($CaV_{1.2}$ and $CaV_{1.3}$) presenting a shifted activation threshold around -30 mV [274] were reported to greatly increase Ca^{2+}-influx at rest.

Box 3: Ca^{2+}-indicators

Ca^{2+}-indicators have long been used to study intracellular [Ca^{2+}] and Ca^{2+}-signaling in living cells. They can be divided into two main classes with advantages and limitations for each: chemical or organic Ca^{2+}-indicators [275] (Indo1, Fura-2, Fluoro4, Oregon Green 488 BAPTA-1: OGB1) and genetically encoded Ca^{2+}-indicators [276] (GECIs: GCaMP6, RGECO).

Chemical Ca^{2+}-indicators have been widely used as Ca^{2+}-sensing fluorescent probes. They can be divided into 2 main classes based on whether they are ratiometric or nonratiometric. Fura-2 is used with excitation ratiometry (dual excitation wavelength, single emission wavelength) whereas Indo-1 is used with emission ratiometry (single excitation wavelength, dual emission wavelength). Their fluorescence is modulated based on the Ca^{2+}-free/Ca^{2+}-bound state. The ratio enables to correct for the local concentration of the Ca^{2+} dye and therefore allows to evaluate the absolute [Ca^{2+}]. Many chemical dyes are available in three chemical forms: salts, dextran conjugates or acetoxymethyl (AM) esters. Salts are the simplest form of Ca^{2+} indicators, but because of their hydrophilic nature, they are membrane impermeable and require invasive loading procedures. They can be introduced into cells by multiple techniques including microinjection, diffusion from patch clamp pipettes, electroporation or lipotransfer using liposomes. As a disadvantage, chemical Ca^{2+}-indicators tend to compartmentalize in membrane-bound structures. Dextran conjugated Ca^{2+} dyes were specifically engineered to address the problem of compartmentalization. Dextrans are very large molecules that have high water solubility and exhibit essentially no compartmentalization. AM esters offer a very convenient method for loading hydrophilic dyes into cells. They are sufficiently hydrophobic to be membrane permeable and get passively loaded into cells. Intracellular esterases cleave off the AM group, thereby trapping the dye in the cytosol. A drawback of ester dyes is their incomplete and heterogeneous cleavage, generating fluorescence from partially cleaved ester indicators, which reduces signal to noise ratio. Generally however, chemical Ca^{2+} indicators offer very good signal-to-noise ratios [277] and can easily be injected in single or small group of neurons by electroporation. The biggest disadvantages of chemical Ca^{2+}-indicators is that they cannot be specifically targeted to a particular organelle and do not allow chronic recordings over several days.

GECIs can be expressed by transfection, viral transduction or transgenesis. The most commonly used GECI is the GCaMP family [278]. GCaMP is built of a circularly permuted green fluorescent protein (cpGFP) fused to calmodulin (CaM) and the CaM-interacting M13 peptide. Ca^{2+}- induced conformational changes in the CaM-M13 complex causes a

brightness increase of the GFP chromophore. GCaMP Ca^{2+} affinity, brightness, and subcellular localization have been improved by mutagenesis on the interface between cpGFP and CaM [279–282] to yield variants with high Ca^{2+} affinity and fast kinetics such as

GCaMP6f [282]. The palette of GECIs expanded to red-shifted (R-GECO, RCaMP) but also blue Ca^{2+}-indicators, facilitating multichannel imaging [283,284]. GECIs are suitable for longitudinal fluorescence imaging over long time periods [285]. GECIs can be used in conjunction with cell-type specific promotors, subcellular targeting sequences or the Cre-LoxP system, facilitating recordings in molecularly identified neuronal types or

subcellular compartments. Significant progress had been made in terms of signal reporting and expression of GECIs but important challenges remain. The use of GECIs in acute slices or *in vivo* requires stereotaxic or *in utero* viral injections which can lead to tissue damage or heterogeneous and unstable expression. In addition, GECIs still present slow Ca^{2+}-association/dissociation kinetics, limiting imaging speed [277] and can potentially lead to cytotoxicity due to long-term expression [286].

Both chemical and genetically encoded Ca^{2+}-indicators present a broad range of Ca^{2+} affinities, association/disassociation kinetics and excitation/emission wavelengths. When selecting an indicator for Ca^{2+} imaging experiments, their Ca^{2+} dependency range, kinetics and their excitation and emission wavelengths need to be considered (see review [287]). In Chapter 2 and 3, we extensively used synthetic Ca^{2+}-indicators (OGB1-AM, Fura2-AM) in comparison with GECIs (GCaMP6s and f) and for ratiometric measurement .

4 Presynaptic plasticity

As detailed in the above sections, many factors influence synaptic activity. As a consequence, synaptic release is highly plastic: dynamically affected by neuronal activity patterns. Synaptic plasticity is controlled by homeostatic mechanisms that dynamically adapt synaptic transmission efficacy in response to various stimuli. Presynaptic homeostatic modulation must be distinguished from postsynaptic modulation which involves neurotransmitter receptor mobility (postsynaptic scaling). Presynaptic homeostatic plasticity is generally induced by neuronal activity via retrograde trans-synaptic signaling that modulates neurotransmitter release [288], presynaptic Ca^{2+} influx [289,290] or vesicular neurotransmitter content [291] among other mechanisms (see review [292]). Synaptic plasticity is crucial for high cognitive functions such as memory, learning and many other behaviors. The next section introduces some key concepts and mechanisms in synaptic plasticity, with a focus on short-term plasticity. Other forms of plasticity exist, but will not be extensively detailed here.

4.1 Synaptic secretion modulation and functional relevance

Long-term synaptic plasticity is a fundamental property of the nervous system. It is commonly considered as the mechanism underlying learning and memory [293,294] (for review [295]). Synapses across the brain present different mechanisms underlying LTP induction.

A common mechanism for long-term potentiation (LTP) arises from the recruitment of postsynaptic AMPA receptors at the PSD or instead the acceleration of their diffusion or removal out of the postsynaptic density [296]. Some studies reported an increase of release probability [297] and LTP [298] mediated by presynaptic NMDA receptors insensitive to Mg^{2+} block (GluN2B, GluN3A subunit). Hippocampal mossy fiber synapses formed from granule cell projections onto postsynaptic cells in the CA3 region present another LTP mechanism mediated by presynaptic autoreceptors (see reviews [299–302]).

Short-term plasticity (STP) also contributes to information processing and allows synapses to perform critical computational functions by acting as a dynamic filter within a neural circuit [303]. This view is supported by studies of cortical and hippocampal circuit operations [304,305]. By this mechanism, the synapses can selectively pass particular information in a feed-forward network. As an example, the information filtering of sensory information in the somatosensory or auditory cortex enables persistent stimulation to be ignored or toned down [305,306] as the result of presynaptic depression during repetitive stimulation.

4.2 Short-term plasticity

The strength of synaptic transmission is shaped by two main properties at the presynaptic element: the probability of vesicular release (P_{vr}) and the number of releasable vesicles in the RRP (RRP size). Those two factors determine together the synaptic probability (Pr) and the synaptic plasticity.

STP occurs within milliseconds to minutes and has predominantly presynaptic origins (Figure 6). Several forms of synaptic short-term plasticity have been identified, including short-term depression (STD) and potentiation (STP). STP is more complex than STD as it occurs in a wider range of time scales. It is classified into facilitation [26,300], augmentation and potentiation (post-tetanic potentiation: PTP ; Figure 6C). Altogether, the multiple components of short-term plasticity interact to perform a variety of synaptic computations for sensory information processing, rapid decision making and working memory [303].

4.2.1 Presynaptic Ca^{2+} dynamics & potentiation

The time course of residual [Ca^{2+}] during and after intense synaptic activity depends on several factors which shape $[Ca^{2+}]_i$ profiles and modulate synaptic strength and plasticity. The different mechanisms include the activity-dependent Ca^{2+} influx from extracellular [307] or intracellular stores [237], the Ca^{2+} buffering or clearance capacity [308]. Presynaptic global buildup of residual Ca^{2+} modulates augmentation and PTP by several distinct processes. Two mechanisms that relate to the work in this thesis are: 1) increasing the size of the RRP through *de novo* synthesis, recruitment and recycling of synaptic vesicles or accelerating priming [135,309,310], or 2) transiently increasing the probability of vesicular release (P_{vr}) [26,41,311–314]. The latest can be mediated by modulation or repositioning of Ca^{2+} sensor proteins among other mechanisms. Those two distinct mechanisms modulate short-term potentiation on different timescales and might respectively mediate PTP and augmentation. The effect of Ca^{2+} buildup through vesicle recruitment or priming (RRP, IRP mediated enhancement) is set up in few seconds, excluding its effectiveness during short interval paired stimuli (Box 4; Figure 6), whereas it should prevail for augmentation and PTP. On the other hand, enhancement of the vesicular release probability likely orchestrates the short-lasting facilitation.

4.2.2 Mechanisms of short-term plasticity

Short-term facilitation (STF) and depression (STD) occur during few to hundreds of milliseconds between subsequent pulses of paired stimulation (Figure 6A). STD is normally attributed to an exhaustion of vesicles in the RRP during a period of repetitive or intense stimulation, when the rate of the pool replenishment by vesicle reuptake and maturation (docking, priming) does not match the speed of vesicle fusion [26,315,316]. Alternatively, repeated short-interval stimulation can facilitate release if vesicular release probability compensates for the loss of releasable vesicles. At most synapses, short-term depression and facilitation co-exist [317,318]. The probability of a vesicle to fuse and release neurotransmitter during a single action potential (vesicular release probability, P_{vr}) at hippocampal synapses is rather low (P_{vr}=0.35) but can vary between different synapses (P_{vr} ~0 to 0.87) [319,320]. A major factor for the balance and change in those forms of synaptic plasticity is the initial release probability (P_r).

Cells presenting a high initial P_r typically display depression [316,321]. The higher the initial P_r is, the higher is the number of vesicles released by a single AP, then depleting a substantial part of the RRP. The RRP is not fully replenished when the next stimulus arrives, giving a smaller number of vesicles to fuse and a smaller EPSC. Consequently, an increase in stimulation frequency (i.e. shortening of the stimulation interval) leads to stronger depression (Box 4; Figure 6). As residual $[Ca^{2+}]_i$ builds up, the release depression is counteracted by an increased rate of vesicle replenishment, fueling the steady-state postsynaptic current. Other forms of depression, relying on postsynaptic processes, exist in parallel to the one described above, such as the saturation of neurotransmitter receptors.

In contrast, synapses with a low initial P_r are likely to facilitate [300] (Box 4; Figure 6A &B). Upon residual Ca^{2+} buildup, the initially low release probability augments, boosting neurotransmitter release in subsequent stimuli. The disparity between peak $[Ca^{2+}]_i$ during exocytosis (up to 100 µM) [54] and residual $[Ca^{2+}]_i$ (10 nM to 300 nM) [218,322] during facilitation is inconsistent with the simplest concept in which a single Ca^{2+} sensor orchestrates both exocytosis and facilitation [323]. This prompt the hypothesis that Ca^{2+} causes facilitation *inter alia* by binding a second class Ca^{2+} sensor with a high Ca^{2+} affinity and slow kinetics distinct from the Ca^{2+} sensor driving fast release [300].

Syt-7 has been implicated in facilitation at Schaffer collateral synapses, hippocampal mossy fiber synapses, corticothalamic synapses and lateral perforant path synapses onto dentate granule cells where Syt-7 is expressed and facilitation is prominent [134]. Paired-pulse facilitation and synaptic enhancement were eliminated in Syt-7 KO and viral expression of wild type but not Ca^{2+}-insensitive mutant of Syt-7 rescued it [134]. Other C_2 domain proteins may be involved in synaptic facilitation. For example, in cultured hippocampal neurons, Doc2 was shown to support short-term enhancement [324], a function which required Ca^{2+} and Munc13 binding.

4.1.2.2 Mechanisms of augmentation and post-tetanic potentiation

Augmentation and potentiation refer to the increase of synaptic strength for tens of seconds to minutes (Figure 6B-C) following high frequency stimulation (HFS). Those two forms of plasticity cannot be measured separately and are together often referred to as post-tetanic potentiation (PTP). However, augmentation may require less intense stimulation than potentiation [26,315] as suggested by the linear relationship between the different forms of plasticity and $[Ca^{2+}]_i$ [312,325].

Intracellular $[Ca^{2+}]$ plays a central role in the induction of augmentation and potentiation [326–328]. Simultaneous measurement of presynaptic $[Ca^{2+}]_i$ or modulation of $[Ca^{2+}]$e together with synaptic information transfer revealed that local $[Ca^{2+}]_i$ at the release site is a major factor that influences synaptic enhancement. Depletion of extracellular Ca^{2+} induces synaptic depression [329] and disrupts long-term potentiation normally developed by train stimulation [330]. Elevation of presynaptic Ca^{2+} accelerates synaptic recovery which is blocked by Ca^{2+} buffering [314,318,331]. Finally, multiple investigations reported that residual bulk $[Ca^{2+}]$ arising from repetitive stimulation affects synaptic potentiation [311–313].
Multiple candidates have been proposed to respond to residual Ca^{2+} to produce augmentation and PTP. Adenylyl cyclase (AC) or phospholipase C (PLC) are activated by $[Ca^{2+}]$ and their activation can potentiate release. The activation of the latter triggers the canonical PLC/DAG pathway (Figure 5). Pharmacology implicated PKC in potentiation at several hippocampal synapses [332,333] and the Calyx of Held synapse [327]. Knockout of calcium-dependent PKC, PKCα and β revealed ~80% reduction of PTP at the calyx of Held [334]. PKC is activated by DAG, which rapidly phosphorylates Munc18-1 [202,335,336] (Figure 5) changing its affinity for syntaxin and vesicle priming. The Ca^{2+} sensor Syt-1 is also phosphorylated by PKC, which induces synaptic transmission potentiation [203] (Figure 5). Munc13-1 and -2 are also implicated in short-term plasticity independently through a residual Ca^{2+} mediated priming mechanism [337,338]. The Munc13-1 dependent potentiation pathway was shown independent of Munc18-1 and PKC but still is mediated by DAG [190,202,339,340]. Altogether, Munc18-1, Munc13-1 and Syt-1 act cooperatively for potentiation through the DAG/PKC pathway (Figure 5). Finally, calmodulin (CaM) dependent upregulation of RRP recovery during high $[Ca^{2+}]$ can also result into potentiation.

The investigation of presynaptic Ca^{2+} dynamics, its effectors and Ca^{2+} sensors for short-term plasticity is a major challenge in neuroscience. A thorough understanding of the mechanisms of interplay between the different pathways is essential for the understanding of information computation by neuron networks, which is the basis of all nervous system function.

Box 4: Electrophysiological paradigms to assess the different forms of synaptic plasticity

Paired Pulse stimulation

A functional aspect of STP can be assessed by electrophysiology using two paired stimuli (Figure 6A), closely spaced with intervals ranging from tens of milliseconds up to seconds. In this thesis, paired pulse paradigms were used extensively with intervals from 20 milliseconds to 1 second (see Figure 6A & chapters 2, 3, 4). Paired-pulse plasticity can be facilitating or depressing, depending on the initial release probability. EPSCs are prone to depress if the initial release is high or to facilitate if the initial P_r is low and global/residual $[Ca^{2+}]_i$ builds-up when the second AP occurs.

Train stimulations

Repetitive stimulation (Figure 4B; Box 1) usually induces depression or synaptic fatigue because the RRP is being emptied faster than replenished [315,316]. However, other forms of depression mechanisms can occur in parallel based on the number of release sites or activity-dependent Ca^{2+} channel inactivation. Residual $[Ca^{2+}]_i$ increases during repeated stimuli accelerate vesicle replenishment, increase Ca^{2+} sensor-dependent vesicle fusion and engender PTP [337,338,341] (Figure 6C). Ca^{2+} build-up depends on many factors including Ca^{2+} buffering capacity, surface Ca^{2+} channel regulation, Ca^{2+} clearance but also Ca^{2+}-induced Ca^{2+}-released (CICR) mechanism and VGCCs [237,238,307,308].

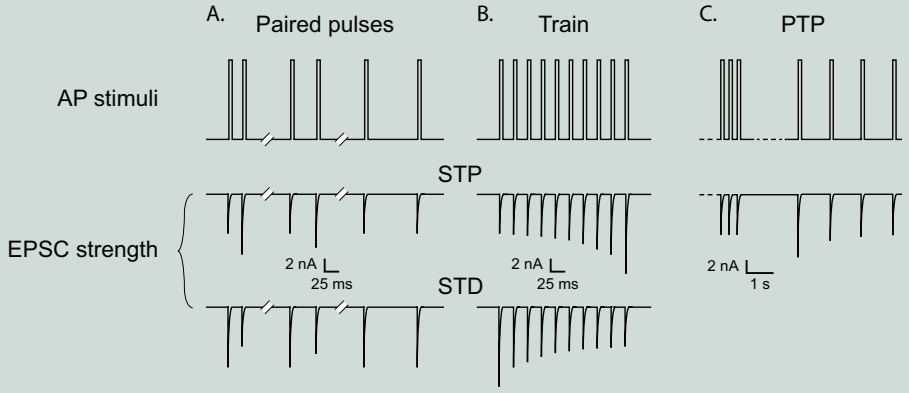

Figure 6: The different forms of presynaptic short-term plasticity. Short-term potentiation (STP) and depression (STD) can be caused by different types of stimulation (depicted in the top images). A. Paired pulse stimulation with various intervals from a few milliseconds to a second can either induce STP (middle panel in A.) or STD (lower panel in A.) depending on the initial release probability (Pr). B. Train stimulation is usually accompanied by synaptic potentiation (middle panel) in neurons with a low initial Pr, but depression (lower panel) in neurons with a high initial Pr. C. High frequency train stimulation (HFS) induces long lasting potentiation know as post-tetanic potentiation (PTP).

5. Aim and outline of the thesis

The general aim of this thesis is to study the role of several Ca^{2+} sensors in evoked and spontaneous neurotransmitter release and their implication in synaptic plasticity. **Chapter 2** and **3** deal with the role of presynaptic fast Ca^{2+}-transients and global $[Ca^{2+}]_i$ rises in resting cells. The second part, **Chapter 4** and **5**, provides insight in the functional involvement of several Ca^{2+} sensors and C_2 domain proteins.

In **chapter 2**, we quantified spontaneous cytosolic Ca^{2+}-transients which appear at rest. Two main classes of Ca^{2+} events were defined: spontaneous Ca^{2+} elevations (SCEs) which comprise all types of Ca^{2+}-events detected under resting conditions, and a subclass of SCEs termed spontaneous Ca^{2+}-transients (SCTs) discernible by their single peak and fast kinetics. We developed a novel method and analysis routine to inspect and quantify short lasting Ca^{2+}-transients (SCTs). Advanced genetically encoded Ca^{2+}-indicators allow to monitor $[Ca^{2+}]_i$ with a high spatial and temporal resolution, offering novel opportunities to identify SCTs but also prompting a need for improved data analysis methods. An algorithm was developed to accurately and automatically identify rapid Ca^{2+} events arising in small cellular compartments, such as the presynaptic element. We demonstrate the reliability of this analysis compared to manual method.
The method was used in **chapter 3** to explore the relation between SCTs and spontaneous glutamate release. Previous evidence indicated that spontaneous release is affected by blockade of voltage-gated Ca^{2+}-channels but also correlated to Ca^{2+} signals originating from intracellular stores, depending on the neuronal type. Using different imaging methods, including GCaMP6 combined with electrophysiology in primary culture of mouse hippocampal neurons, we studied the regulation of mEPSCs by extracellular and intracellular $[Ca^{2+}]$. We found no strong evidence for a tight coupling of stochastic Ca^{2+} elevations to mEPSCs in this neuronal preparation, suggesting that spontaneous neurotransmitter release events are governed by global $[Ca^{2+}]_i$ levels or, alternatively, are coupled to spontaneous Ca^{2+} elevations by a slow (>1s) or temporally variable mechanism.

Chapter 4 focuses on the phenotypic effect of Doc2b Ca^{2+}-binding site mutations on spontaneous and evoked neurotransmitter release in primary cultures of hippocampal neurons. In previous studies, two Doc2b mutants $Doc2b^{DN}$ and $Doc2b^{6A}$ (which carry the substitutions D218,220N or D163,218,220,303,357,359A respectively) have respectively been classified as gain- and loss-of functions and this has led to different interpretations of Doc2b's function as a Ca^{2+} sensor or not [133,138]. In a side-by-side comparison, both mutants similarly affected Ca^{2+}-dependent membrane binding as well as synaptic function. We revealed a potential function for the protein in short-term plasticity release during and after high frequency stimulation and reconciled conflicting data concerning its effect for spontaneous release.

Chapter 5 extends our study on spontaneous release, aiming to elucidate additional C_2 domain proteins responsible for the remaining spontaneous release in absence of the main sensors Doc2a/b.

Using null mouse models for Doc2c, Rabphilin3A and Synaptotagmin-7, we found that Doc2c and Synaptotagmin-7 do not regulate mEPSCs, while a potential effect for Rabphilin3A appeared in glutamatergic spontaneous release specifically in network cultures of hippocampal neurons.

Finally, **Chapter 6** provides a general discussion on new experimental findings and procedures that apply to the scope of our research, in the context of existing literature. A detailed discussion in given on the relevance of spatial Ca^{2+}-events which may potentially lead to spontaneous release. Finally, this chapter puts forward newly emerging questions and perspectives that arise from the thesis, which could be the basis for future investigations.

References

1. Hodgkin, A. L. & Huxley, A. F. A quantitative description of membrane current and its application to conduction and excitation in nerve. J. Physiol. 117, 500–544 (1952).
2. Herculano-Houzel, S. The human brain in numbers: a linearly scaled-up primate brain. Front. Hum. Neurosci. 3, 31 (2009).
3. von Bartheld, C. S., Bahney, J. & Herculano-Houzel, S. The search for true numbers of neurons and glial cells in the human brain: A review of 150 years of cell counting. J. Comp. Neurol. 524, 3865–3895 (2016).
4. Rizzoli, S. O. Synaptic vesicle recycling: steps and principles. EMBO J. 33, 788–822 (2014).
5. Südhof, T. C. The synaptic vesicle cycle. Annu. Rev. Neurosci. 27, 509–47 (2004).
6. Stadler, H. & Tsukita, S. Synaptic vesicles contain an ATP-dependent proton pump and show 'knob-like' protrusions on their surface. EMBO J. 3, 3333–7 (1984).
7. Maycox, P. R., Deckwerth, T., Hell, J. W. & Jahn, R. Glutamate uptake by brain synaptic vesicles. Energy dependence of transport and functional reconstitution in proteoliposomes. J. Biol. Chem. 263, 15423–8 (1988).
8. Bucci, M. How to fill a vesicle. Nat. Chem. Biol. 7, 654–654 (2011).
9. Milovanovic, D., Wu, Y., Bian, X. & De Camilli, P. A liquid phase of synapsin and lipid vesicles. Science (80-.). 361, 604–607 (2018).
10. Milovanovic, D. & De Camilli, P. Synaptic Vesicle Clusters at Synapses: A Distinct Liquid Phase? Neuron 93, 995–1002 (2017).
11. Ghelani, T. & Sigrist, S. J. Coupling the Structural and Functional Assembly of Synaptic Release Sites. Front. Neuroanat. 12, 81 (2018).
12. Südhof, T. C. Review The Presynaptic Active Zone. Neuron 75, 11–25 (2012).
13. Held, R. G. & Kaeser, P. S. ELKS active zone proteins as multitasking scaffolds for secretion. Open Biol. 8, (2018).
14. Baydyuk, M., Xu, J. & Wu, L.-G. The calyx of Held in the auditory system: Structure, function, and development. Hear. Res. 338, 22–31 (2016).
15. Matthews, G. & Fuchs, P. The diverse roles of ribbon synapses in sensory neurotransmission. Nat. Rev. Neurosci. 11, 812–22 (2010).
16. Takamori, S. et al. Molecular anatomy of a trafficking organelle. Cell 127, 831–46 (2006).
17. Pulido, C., Trigo, F. F., Llano, I. & Marty, A. Vesicular Release Statistics and Unitary Postsynaptic Current at Single GABAergic Synapses. Neuron 85, 159–172 (2015).
18. Malagon, G., Miki, T., Tran, V., Gomez, L. C. & Marty, A. Incomplete vesicular docking limits synaptic strength under high release probability conditions. Elife 9, (2020).
19. Pulido, C. & Marty, A. Quantal Fluctuations in Central Mammalian Synapses: Functional Role of Vesicular Docking Sites. Physiol. Rev. 97, 1403–1430 (2017).
20. Trigo, F. F., Sakaba, T., Ogden, D. & Marty, A. Readily releasable pool of synaptic vesicles measured at single synaptic contacts. Proc. Natl. Acad. Sci. 109, 18138–18143 (2012).
21. Borges-Merjane, C., Kim, O. & Jonas, P. Functional Electron Microscopy, "Flash and Freeze," of Identified Cortical Synapses in Acute Brain Slices. Neuron 105, 992-1006.e6 (2020).
22. de Wit, H. et al. Synaptotagmin-1 docks secretory vesicles to syntaxin-1/SNAP-25 acceptor complexes. Cell 138, 935–46 (2009).
23. Chang, S., Trimbuch, T. & Rosenmund, C. Synaptotagmin-1 drives synchronous Ca^{2+}-triggered fusion by C2B-domain-mediated synaptic-vesicle-membrane attachment. Nat. Neurosci. 21, 33–40 (2018).
24. Vandael, D., Borges-Merjane, C., Zhang, X. & Jonas, P. Short-Term Plasticity at Hippocampal Mossy Fiber Synapses Is Induced by Natural Activity Patterns and Associated with Vesicle Pool Engram Formation. Neuron 107, 509-521.e7 (2020).
25. Südhof, T. C. The Synaptic Vesicle Cycle Revisited. Neuron 28, 317–320 (2000).
26. Zucker, R. S. & Regehr, W. G. Short-term synaptic plasticity. Annu. Rev. Physiol. 64, 355–405 (2002).
27. Rizzoli, S. O. & Betz, W. J. Synaptic vesicle pools. Nat. Rev. Neurosci. 6, 57–69 (2005).
28. Alabi, A. A. & Tsien, R. W. Synaptic vesicle pools and dynamics. Cold Spring Harb. Perspect. Biol. 4, a013680 (2012).
29. Chamberland, S. & Tóth, K. Functionally heterogeneous synaptic vesicle pools support diverse synaptic signalling. J. Physiol. 594, 825–835 (2016).
30. Murthy, V. N. & Stevens, C. F. Reversal of synaptic vesicle docking at central synapses. Nat. Neurosci. 2, 503–7 (1999).
31. Fernandez-Alfonso, T. & Ryan, T. A. A heterogeneous 'resting' pool of synaptic vesicles that is dynamically interchanged across boutons in mammalian CNS synapses. Brain Cell Biol. 36, 87–100 (2008).

32. Ratnayaka, A. et al. Recruitment of resting vesicles into recycling pools supports NMDA receptor-dependent synaptic potentiation in cultured hippocampal neurons. J. Physiol. 590, 1585–97 (2012).
33. Kuromi, H. & Kidokoro, Y. Selective replenishment of two vesicle pools depends on the source of Ca^{2+} at the Drosophila synapse. Neuron 35, 333–43 (2002).
34. Fredj, N. Ben & Burrone, J. A resting pool of vesicles is responsible for spontaneous vesicle fusion at the synapse. Nat. Neurosci. 12, 751–8 (2009).
35. Neher, E. Merits and Limitations of Vesicle Pool Models in View of Heterogeneous Populations of Synaptic Vesicles. Neuron 87, 1131–1142 (2015).
36. Horrigan, F. T. & Bookman, R. J. Releasable pools and the kinetics of exocytosis in adrenal chromaffin cells. Neuron 13, 1119–29 (1994).
37. Alvarez, Y. D. & Marengo, F. D. The immediately releasable vesicle pool: highly coupled secretion in chromaffin and other neuroendocrine cells. J. Neurochem. 116, 155–63 (2011).
38. Schlüter, O. M., Basu, J., Südhof, T. C. & Rosenmund, C. Rab3 superprimes synaptic vesicles for release: implications for short-term synaptic plasticity. J. Neurosci. 26, 1239–46 (2006).
39. Lee, J. S., Ho, W.-K., Neher, E. & Lee, S.-H. Superpriming of synaptic vesicles after their recruitment to the readily releasable pool. Proc. Natl. Acad. Sci. U. S. A. 110, 15079–84 (2013).
40. Goda, Y. & Stevens, C. F. Readily releasable pool size changes associated with long term depression. Proc. Natl. Acad. Sci. 95, 1283–1288 (1998).
41. Branco, T., Marra, V. & Staras, K. Examining size–strength relationships at hippocampal synapses using an ultrastructural measurement of synaptic release probability. J. Struct. Biol. 172, 203–210 (2010).
42. Rey, S., Marra, V., Smith, C. & Staras, K. Nanoscale Remodeling of Functional Synaptic Vesicle Pools in Hebbian Plasticity. Cell Rep. 30, 2006-2017.e3 (2020).
43. Lee, J. S., Ho, W.-K. & Lee, S.-H. Post-tetanic increase in the fast-releasing synaptic vesicle pool at the expense of the slowly releasing pool. J. Gen. Physiol. 136, 259–72 (2010).
44. Dresbach, T., Qualmann, B., Kessels, M. M., Garner, C. C. & Gundelfinger, E. D. The presynaptic cytomatrix of brain synapses. Cell. Mol. Life Sci. 58, 94–116 (2001).
45. Neher, E. & Brose, N. Dynamically Primed Synaptic Vesicle States: Key to Understand Synaptic Short-Term Plasticity. Neuron 100, 1283–1291 (2018).
46. Wojcik, S. M. & Brose, N. Regulation of Membrane Fusion in Synaptic Excitation-Secretion Coupling: Speed and Accuracy Matter. Neuron 55, 11–24 (2007).
47. Verhage, M. & Sørensen, J. B. Vesicle docking in regulated exocytosis. Traffic 9, 1414–1424 (2008).
48. Hallermann, S. et al. Bassoon speeds vesicle reloading at a central excitatory synapse. Neuron 68, 710–23 (2010).
49. Saviane, C. & Silver, R. A. Fast vesicle reloading and a large pool sustain high bandwidth transmission at a central synapse. Nature 439, 983–7 (2006).
50. Sätzler, K. et al. Three-dimensional reconstruction of a calyx of Held and its postsynaptic principal neuron in the medial nucleus of the trapezoid body. J. Neurosci. 22, 10567–79 (2002).
51. Schikorski, T. & Stevens, C. F. Morphological correlates of functionally defined synaptic vesicle populations. Nat. Neurosci. 4, 391–5 (2001).
52. Taschenberger, H., Leão, R. M., Rowland, K. C., Spirou, G. A. & von Gersdorff, H. Optimizing synaptic architecture and efficiency for high-frequency transmission. Neuron 36, 1127–43 (2002).
53. Varoqueaux, F. et al. Total arrest of spontaneous and evoked synaptic transmission but normal synaptogenesis in the absence of Munc13-mediated vesicle priming. Proc. Natl. Acad. Sci. 99, 9037–9042 (2002).
54. Nakamura, Y. et al. Nanoscale Distribution of Presynaptic Ca^{2+} Channels and Its Impact on Vesicular Release during Development. Neuron 85, 145–158 (2015).
55. Wolfel, M., Lou, X. & Schneggenburger, R. A Mechanism Intrinsic to the Vesicle Fusion Machinery Determines Fast and Slow Transmitter Release at a Large CNS Synapse. J. Neurosci. 27, 3198–3210 (2007).
56. Zhang, Q., Li, Y. & Tsien, R. W. The Dynamic Control of Kiss-And-Run and Vesicular Reuse Probed with Single Nanoparticles. Science (80-.). 323, 1448–1453 (2009).
57. Valtorta, F., Meldolesi, J. & Fesce, R. Synaptic vesicles: is kissing a matter of competence? Trends Cell Biol. 11, 324–8 (2001).
58. Alés, E. et al. High calcium concentrations shift the mode of exocytosis to the kiss-and-run mechanism. Nat. Cell Biol. 1, 40–4 (1999).
59. Wu, W., Xu, J., Wu, X.-S. & Wu, L.-G. Activity-dependent acceleration of endocytosis at a central synapse. J. Neurosci. 25, 11676–83 (2005).
60. Watanabe, S. et al. Ultrafast endocytosis at Caenorhabditis elegans neuromuscular junctions. Elife 2, e00723 (2013).

61. Watanabe, S. et al. Ultrafast endocytosis at mouse hippocampal synapses. Nature 504, 242–247 (2013).
62. He, L. & Wu, L.-G. The debate on the kiss-and-run fusion at synapses. Trends Neurosci. 30, 447–55 (2007).
63. Stevens, C. F. & Williams, J. H. 'Kiss and run' exocytosis at hippocampal synapses. Proc. Natl. Acad. Sci. U. S. A. 97, 12828–33 (2000).
64. Taschenberger, H., Woehler, A. & Neher, E. Superpriming of synaptic vesicles as a common basis for intersynapse variability and modulation of synaptic strength. Proc. Natl. Acad. Sci. U. S. A. 113, E4548-57 (2016).
65. Poirier, M. A. et al. The synaptic SNARE complex is a parallel four-stranded helical bundle. Nat. Struct. Biol. 5, 765–769 (1998).
66. Sutton, R. B., Fasshauer, D., Jahn, R. & Brunger, A. T. Crystal structure of a SNARE complex involved in synaptic exocytosis at 2.4 A resolution. Nature 395, 347–53 (1998).
67. Yoon, T.-Y. & Munson, M. SNARE complex assembly and disassembly. Curr. Biol. 28, R397–R401 (2018).
68. Sørensen, J. B. et al. Sequential N- to C-terminal SNARE complex assembly drives priming and fusion of secretory vesicles. EMBO J. 25, 955–966 (2006).
69. Jahn, R. & Fasshauer, D. Molecular machines governing exocytosis of synaptic vesicles. Nature 490, 201–207 (2012).
70. Mohrmann, R. & Sørensen, J. B. SNARE requirements en route to exocytosis: From many to few. J. Mol. Neurosci. 48, 387–394 (2012).
71. Gao, Y. et al. Single Reconstituted Neuronal SNARE Complexes Zipper in Three Distinct Stages. Science (80-.). 337, 1340–1343 (2012).
72. Mohrmann, R., de Wit, H., Verhage, M., Neher, E. & Sørensen, J. B. Fast vesicle fusion in living cells requires at least three SNARE complexes. Science 330, 502–5 (2010).
73. Brunger, A. T. et al. The pre-synaptic fusion machinery. Curr. Opin. Struct. Biol. 54, 179–188 (2019).
74. Brenner, S. The genetics of Caenorhabditis elegans. Genetics 77, 71–94 (1974).
75. Hosono, R. et al. The unc-18 gene encodes a novel protein affecting the kinetics of acetylcholine metabolism in the nematode Caenorhabditis elegans. J. Neurochem. 58, 1517–25 (1992).
76. Verhage, M. et al. Synaptic assembly of the brain in the absence of neurotransmitter secretion. Science 287, 864–9 (2000).
77. Gulyás-Kovács, A. et al. Munc18-1: sequential interactions with the fusion machinery stimulate vesicle docking and priming. J. Neurosci. 27, 8676–86 (2007).
78. Hata, Y., Slaughter, C. A. & Südhof, T. C. Synaptic vesicle fusion complex contains unc-18 homologue bound to syntaxin. Nature 366, 347–351 (1993).
79. Xu, Y., Su, L. & Rizo, J. Binding of Munc18-1 to Synaptobrevin and to the SNARE Four-Helix Bundle. Biochemistry 49, 1568–1576 (2010).
80. Dulubova, I. A conformational switch in syntaxin during exocytosis: role of munc18. EMBO J. 18, 4372–4382 (1999).
81. Stepien, K. P., Prinslow, E. A. & Rizo, J. Munc18-1 is crucial to overcome the inhibition of synaptic vesicle fusion by αSNAP. Nat. Commun. 10, 4326 (2019).
82. Verhage, M. et al. DOC2 proteins in rat brain: complementary distribution and proposed function as vesicular adapter proteins in early stages of secretion. Neuron 18, 453–61 (1997).
83. Novick, P. & Schekman, R. Secretion and cell-surface growth are blocked in a temperature-sensitive mutant of Saccharomyces cerevisiae. Proc. Natl. Acad. Sci. U. S. A. 76, 1858–62 (1979).
84. Garcia, E. P., Gatti, E., Butler, M., Burton, J. & De Camilli, P. A rat brain Sec1 homologue related to Rop and UNC18 interacts with syntaxin. Proc. Natl. Acad. Sci. U. S. A. 91, 2003–7 (1994).
85. Pevsner, J., Hsu, S. C. & Scheller, R. H. n-Sec1: a neural-specific syntaxin-binding protein. Proc. Natl. Acad. Sci. U. S. A. 91, 1445–9 (1994).
86. Augustin, I., Rosenmund, C., Südhof, T. C. & Brose, N. Munc13-1 is essential for fusion competence of glutamatergic synaptic vesicles. Nature 400, 457–61 (1999).
87. Fernandez, I. et al. Three-dimensional structure of an evolutionarily conserved N-terminal domain of syntaxin 1A. Cell 94, 841–9 (1998).
88. Burkhardt, P., Hattendorf, D. A., Weis, W. I. & Fasshauer, D. Munc18a controls SNARE assembly through its interaction with the syntaxin N-peptide. EMBO J. 27, 923–933 (2008).
89. Ma, C., Su, L., Seven, A. B., Xu, Y. & Rizo, J. Reconstitution of the vital functions of Munc18 and Munc13 in neurotransmitter release. Science 339, 421–425 (2013).
90. Ma, C., Li, W., Xu, Y. & Rizo, J. Munc13 mediates the transition from the closed syntaxin-Munc18 complex to the SNARE complex. Nat. Struct. Mol. Biol. 18, 542–549 (2011).
91. Wang, S. et al. Conformational change of syntaxin linker region induced by Munc13s initiates SNARE complex formation in synaptic exocytosis. EMBO J. 36, 816–829 (2017).

92. Wang, S. et al. Munc18 and Munc13 serve as a functional template to orchestrate neuronal SNARE complex assembly. Nat. Commun. 10, 69 (2019).
93. Richmond, J. E., Weimer, R. M. & Jorgensen, E. M. An open form of syntaxin bypasses the requirement for UNC-13 in vesicle priming. Nature 412, 338–41 (2001).
94. Shu, T., Jin, H., Rothman, J. E. & Zhang, Y. Munc13-1 MUN domain and Munc18-1 cooperatively chaperone SNARE assembly through a tetrameric complex. Proc. Natl. Acad. Sci. 117, 1036–1041 (2020).
95. Lai, Y. et al. Molecular Mechanisms of Synaptic Vesicle Priming by Munc13 and Munc18. Neuron 95, 591-607. e10 (2017).
96. Quade, B. et al. Membrane bridging by Munc13-1 is crucial for neurotransmitter release. Elife 8, (2019).
97. He, E. et al. Munc13-1 and Munc18-1 together prevent NSF-dependent de-priming of synaptic vesicles. Nat Commun 8, 15915 (2017).
98. Junge, H. J. et al. Calmodulin and Munc13 Form a Ca^{2+} Sensor/Effector Complex that Controls Short-Term Synaptic Plasticity. Cell 118, 389–401 (2004).
99. Reim, K. et al. Complexins regulate a late step in Ca^{2+}-dependent neurotransmitter release. Cell 104, 71–81 (2001).
100. Tang, J. et al. A Complexin/Synaptotagmin 1 Switch Controls Fast Synaptic Vesicle Exocytosis. Cell 126, 1175–1187 (2006).
101. Chen, X. et al. Three-Dimensional Structure of the Complexin/SNARE Complex. Neuron 33, 397–409 (2002).
102. Chang, S. et al. Complexin Stabilizes Newly Primed Synaptic Vesicles and Prevents Their Premature Fusion at the Mouse Calyx of Held Synapse. J. Neurosci. 35, 8272–8290 (2015).
103. Fujita, Y. et al. Tomosyn: A syntaxin-1-binding protein that forms a novel complex in the neurotransmitter release process. Neuron 20, 905–915 (1998).
104. Scales, S. J., Hesser, B. A., Masuda, E. S. & Scheller, R. H. Amisyn, a novel syntaxin-binding protein that may regulate SNARE complex assembly. J. Biol. Chem. 277, 28271–9 (2002).
105. Shin, O.-H. Exocytosis and synaptic vesicle function. Compr. Physiol. 4, 149–75 (2014).
106. Rizo, J. & Sudhof, T. C. C2-domains, structure and function of a universal Ca^{2+}-binding domain. J. Biol. Chem. 273, 15879–15882 (1998).
107. Tanaka, C. & Nishizuka, Y. The Protein Kinase C Family for Neuronal Signaling. Annu. Rev. Neurosci. 17, 551–567 (1994).
108. Leonard, T. A. C2 Domain Proteins. in Encyclopedia of Metalloproteins 309–318 (Springer New York, 2013). doi:10.1007/978-1-4614-1533-6_39
109. Alwarawrah, M. & Wereszczynski, J. Investigation of the Effect of Bilayer Composition on PKCα-C2 Domain Docking Using Molecular Dynamics Simulations. J. Phys. Chem. B 121, 78–88 (2017).
110. Nikolaus, J., Warner, J. M., O'shaughnessy, B. & Herrmann, A. C2 Domains and Membrane Fusion. Membr. Fusion 68, 1–32 (2011).
111. Martens, S., Kozlov, M. M. & McMahon, H. T. How synaptotagmin promotes membrane fusion. Science 316, 1205–8 (2007).
112. Sabatini, B. L. & Regehr, W. G. Timing of neurotransmission at fast synapses in the mammalian brain. Nature 384, 170–2 (1996).
113. Katz, B. Quantal mechanism of neural transmitter release. Science 173, 123–6 (1971).
114. Maximov, A. Synaptotagmins. in Encyclopedia of Neuroscience 819–821 (Elsevier, 2009). doi:10.1016/B978-008045046-9.01358-9
115. Chen, C. & Jonas, P. Synaptotagmins: That's Why So Many. Neuron 94, 694–696 (2017).
116. Xu, J., Mashimo, T. & Südhof, T. C. Synaptotagmin-1, -2, and -9: Ca^{2+} Sensors for Fast Release that Specify Distinct Presynaptic Properties in Subsets of Neurons. Neuron 54, 567–581 (2007).
117. Bacaj, T. et al. Synaptotagmin-1 and Synaptotagmin-7 Trigger Synchronous and Asynchronous Phases of Neurotransmitter Release. Neuron 80, 947–959 (2013).
118. Geppert, M. et al. Synaptotagmin I: a major Ca^{2+} sensor for transmitter release at a central synapse. Cell 79, 717–27 (1994).
119. Nishiki, T. -i. Synaptotagmin I Synchronizes Transmitter Release in Mouse Hippocampal Neurons. J. Neurosci. 24, 6127–6132 (2004).
120. Sun, J. et al. A dual-Ca^{2+}-sensor model for neurotransmitter release in a central synapse. Nature 450, 676–82 (2007).
121. Pang, Z. P. et al. Synaptotagmin-2 is essential for survival and contributes to Ca^{2+} triggering of neurotransmitter release in central and neuromuscular synapses. J. Neurosci. 26, 13493–504 (2006).
122. Ubach, J., Zhang, X., Shao, X., Südhof, T. C. & Rizo, J. Ca^{2+} binding to synaptotagmin: how many Ca^{2+} ions bind to the tip of a C2-domain? EMBO J. 17, 3921–3930 (1998).

123. Fernandez, I. et al. Three-dimensional structure of the synaptotagmin 1 C2B-domain: Synaptotagmin 1 as a phospholipid binding machine. Neuron 32, 1057–1069 (2001).
124. Shao, X., Fernandez, I., Südhof, T. C. & Rizo, J. Solution Structures of the Ca^{2+} -free and Ca^{2+}-bound C2A Domain of Synaptotagmin I: Does Ca^{2+} Induce a Conformational Change? Biochemistry 37, 16106–16115 (1998).
125. Araç, D. et al. Close membrane-membrane proximity induced by Ca^{2+}-dependent multivalent binding of synaptotagmin-1 to phospholipids. Nat. Struct. Mol. Biol. 13, 209–217 (2006).
126. Zhou, Q. et al. The primed SNARE–complexin–synaptotagmin complex for neuronal exocytosis. Nature 548, 420–425 (2017).
127. Brunger, A. T., Leitz, J., Zhou, Q., Choi, U. B. & Lai, Y. Ca^{2+}-Triggered Synaptic Vesicle Fusion Initiated by Release of Inhibition. Trends Cell Biol. 28, 631–645 (2018).
128. Hui, E., Johnson, C. P., Yao, J., Dunning, F. M. & Chapman, E. R. Synaptotagmin-mediated bending of the target membrane is a critical step in $Ca^{(2+)}$-regulated fusion. Cell 138, 709–21 (2009).
129. Lynch, K. L. et al. Synaptotagmin-1 utilizes membrane bending and SNARE binding to drive fusion pore expansion. Mol. Biol. Cell 19, 5093–103 (2008).
130. Luo, F. & Südhof, T. C. Synaptotagmin-7-Mediated Asynchronous Release Boosts High-Fidelity Synchronous Transmission at a Central Synapse. Neuron 94, 826-839.e3 (2017).
131. Luo, F., Bacaj, T. & Südhof, T. C. Synaptotagmin-7 Is Essential for Ca^{2+}-Triggered Delayed Asynchronous Release But Not for Ca^{2+}-Dependent Vesicle Priming in Retinal Ribbon Synapses. J. Neurosci. 35, 11024–11033 (2015).
132. Chen, C., Satterfield, R., Young, S. M. & Jonas, P. Triple Function of Synaptotagmin 7 Ensures Efficiency of High-Frequency Transmission at Central GABAergic Synapses. Cell Rep. 21, 2082–2089 (2017).
133. Pang, Z. P. et al. Doc2 supports spontaneous synaptic transmission by a $Ca^{(2+)}$-independent mechanism. Neuron 70, 244–51 (2011).
134. Jackman, S. L., Turecek, J., Belinsky, J. E. & Regehr, W. G. The calcium sensor synaptotagmin 7 is required for synaptic facilitation. Nature 529, 88–91 (2016).
135. Liu, H. et al. Synaptotagmin 7 functions as a Ca^{2+}-sensor for synaptic vesicle replenishment. Elife 3, e01524 (2014).
136. Tokumaru, H., Shimizu-Okabe, C. & Abe, T. Direct interaction of SNARE complex binding protein synaphin/complexin with calcium sensor synaptotagmin 1. Brain Cell Biol. 36, 173–89 (2008).
137. Lai, Y. et al. Complexin inhibits spontaneous release and synchronizes Ca^{2+}-triggered synaptic vesicle fusion by distinct mechanisms. Elife 3, e03756 (2014).
138. Groffen, A. J. et al. Doc2b Is a High-Affinity Ca^{2+} Sensor for Spontaneous Neurotransmitter Release. Science (80-.). 327, 1614–1618 (2010).
139. Courtney, N. A., Briguglio, J. S., Bradberry, M. M., Greer, C. & Chapman, E. R. Excitatory and Inhibitory Neurons Utilize Different Ca^{2+} Sensors and Sources to Regulate Spontaneous Release. Neuron 98, 977-991.e5 (2018).
140. Giladi, M. et al. The C2B domain is the primary Ca^{2+} sensor in DOC2B: a structural and functional analysis. J. Mol. Biol. 425, 4629–4641 (2013).
141. Gaffaney, J. D., Xue, R. & Chapman, E. R. Mutations that disrupt Ca^{2+}-binding activity endow Doc2β with novel functional properties during synaptic transmission. Mol. Biol. Cell 25, 481–494 (2014).
142. Friedrich, R. et al. DOC2B acts as a calcium switch and enhances vesicle fusion. J Neurosci 28, 6794–6806 (2008).
143. Groffen, A. J. A., Friedrich, R., Brian, E. C., Ashery, U. & Verhage, M. DOC2A and DOC2B are sensors for neuronal activity with unique calcium-dependent and kinetic properties. J. Neurochem. 97, 818–833 (2006).
144. Sugita, S., Shin, O.-H., Han, W., Lao, Y. & Südhof, T. C. Synaptotagmins form a hierarchy of exocytotic $Ca^{(2+)}$ sensors with distinct $Ca^{(2+)}$ affinities. EMBO J. 21, 270–80 (2002).
145. Guillén, J. et al. Structural insights into the Ca^{2+} and PI(4,5)P2 binding modes of the C2 domains of rabphilin 3A and synaptotagmin 1. Proc. Natl. Acad. Sci. U. S. A. 110, 20503–8 (2013).
146. Honigmann, A. et al. Phosphatidylinositol 4,5-bisphosphate clusters act as molecular beacons for vesicle recruitment. Nat. Struct. Mol. Biol. 20, 679–86 (2013).
147. Sato, M. et al. Role of the polybasic sequence in the Doc2alpha C2B domain in dense-core vesicle exocytosis in PC12 cells. J. Neurochem. 114, 171–81 (2010).
148. Yao, J., Gaffaney, J. D., Kwon, S. E. & Chapman, E. R. Doc2 is a Ca^{2+} sensor required for asynchronous neurotransmitter release. Cell 147, 666–77 (2011).
149. Xue, R., Gaffaney, J. D. & Chapman, E. R. Structural elements that underlie Doc2β function during asynchronous synaptic transmission. Proc. Natl. Acad. Sci. 112, 201502288 (2015).
150. Houy, S. et al. Doc2B acts as a calcium sensor for vesicle priming requiring synaptotagmin-1, Munc13-2 and SNAREs. Elife 6, (2017).
151. Bourgeois-Jaarsma, Q., Verhage, M. & Groffen, A. J. Doc2b Ca^{2+} binding site mutants enhance synaptic release

at rest at the expense of sustained synaptic strength. Sci. Rep. 9, 14408 (2019).
152. Volynski, K. E. & Krishnakumar, S. S. Synergistic control of neurotransmitter release by different members of the synaptotagmin family. Curr. Opin. Neurobiol. 51, 154–162 (2018).
153. Walter, A. M., Groffen, A. J., Sørensen Jakob B., J. B. & Verhage, M. Multiple Ca^{2+} sensors in secretion: Teammates, competitors or autocrats? Trends Neurosci. 34, 487–497 (2011).
154. Pang, Z. P. et al. Genetic analysis of synaptotagmin 2 in spontaneous and Ca^{2+}-triggered neurotransmitter release. EMBO J. 25, 2039–2050 (2006).
155. Littleton, J. T. T., Stern, M., Schulze, K., Perin, M. & Bellen, H. J. Mutational analysis of Drosophila synaptotagmin demonstrates its essential role in $Ca(^{2+})$-activated neurotransmitter release. Cell 74, 1125–34 (1993).
156. Xu, J., Pang, Z. P., Shin, O. & Südhof, T. C. Synaptotagmin-1 functions as a Ca^{2+} sensor for spontaneous release. Nat. Neurosci. 12, 759–766 (2009).
157. Kochubey, O. & Schneggenburger, R. Synaptotagmin increases the dynamic range of synapses by driving Ca^{2+}-evoked release and by clamping a near-linear remaining Ca^{2+} sensor. Neuron 69, 736–48 (2011).
158. Liu, H., Dean, C., Arthur, C. P., Dong, M. & Chapman, E. R. Autapses and networks of hippocampal neurons exhibit distinct synaptic transmission phenotypes in the absence of synaptotagmin I. J. Neurosci. 29, 7395–7403 (2009).
159. Broadie, K., Bellen, H. J., DiAntonio, A., Littleton, J. T. & Schwarz, T. L. Absence of synaptotagmin disrupts excitation-secretion coupling during synaptic transmission. Proc. Natl. Acad. Sci. U. S. A. 91, 10727–31 (1994).
160. Turecek, J., Jackman, S. L. & Regehr, W. G. Synaptotagmin 7 confers frequency invariance onto specialized depressing synapses. Nature 551, 503–506 (2017).
161. Díez-Arazola, R. et al. Doc2 proteins are not required for the increased spontaneous release rate in synaptotagmin-1 deficient neurons. J. Neurosci. (2020). doi:10.1523/JNEUROSCI.0309-19.2020
162. Vasin, A., Volfson, D., Littleton, J. T. & Bykhovskaia, M. Interaction of the Complexin Accessory Helix with Synaptobrevin Regulates Spontaneous Fusion. Biophys. J. 111, 1954–1964 (2016).
163. Xue, M. et al. Distinct domains of complexin I differentially regulate neurotransmitter release. Nat. Struct. Mol. Biol. 14, 949–58 (2007).
164. Simons, K. & Toomre, D. Lipid rafts and signal transduction. Nat. Rev. Mol. Cell Biol. 1, 31–9 (2000).
165. Chernomordik, L. V. & Kozlov, M. M. Protein-Lipid Interplay in Fusion and Fission of Biological Membranes. Annu. Rev. Biochem. 72, 175–207 (2003).
166. Rohrbough, J. & Broadie, K. Lipid regulation of the synaptic vesicle cycle. Nat. Rev. Neurosci. 6, 139–150 (2005).
167. Breckenridge, W. C., Gombos, G. & Morgan, I. G. The lipid composition of adult rat brain synaptosomal plasma membranes. Biochim. Biophys. Acta 266, 695–707 (1972).
168. Boesze-Battaglia, K. & Schimmel, R. Cell membrane lipid composition and distribution: implications for cell function and lessons learned from photoreceptors and platelets. J. Exp. Biol. 200, 2927–36 (1997).
169. Lewis, K. T., Maddipati, K. R., Taatjes, D. J. & Jena, B. P. Neuronal porosome lipidome. J. Cell. Mol. Med. 18, 1927–37 (2014).
170. Putta, P. et al. Phosphatidic acid binding proteins display differential binding as a function of membrane curvature stress and chemical properties. Biochim. Biophys. Acta - Biomembr. 1858, 2709–2716 (2016).
171. Gaffaney, J. D., Dunning, F. M., Wang, Z., Hui, E. & Chapman, E. R. Synaptotagmin C2B Domain Regulates Ca^{2+}-triggered Fusion in Vitro. J. Biol. Chem. 283, 31763–31775 (2008).
172. Svennerholm, L. Distribution and fatty acid composition of phosphoglycerides in normal human brain. J. Lipid Res. 9, 570–9 (1968).
173. Fadok, V. A. et al. Exposure of phosphatidylserine on the surface of apoptotic lymphocytes triggers specific recognition and removal by macrophages. J. Immunol. 148, 2207–16 (1992).
174. Zhang, W., Stetler, R. A. & Chen, J. Akt-GSK3β Pro-survival Signaling Pathway in Cerebral Ischemic Injury. in Primer on Cerebrovascular Diseases 269–272 (Elsevier, 2017). doi:10.1016/B978-0-12-803058-5.00055-2
175. Kim, H.-Y., Huang, B. X. & Spector, A. A. Phosphatidylserine in the brain: Metabolism and function. Prog. Lipid Res. 56, 1–18 (2014).
176. Kuo, W., Herrick, D. Z., Ellena, J. F. & Cafiso, D. S. The Calcium-Dependent and Calcium-Independent Membrane Binding of Synaptotagmin 1: Two Modes of C2B Binding. J. Mol. Biol. 387, 284–294 (2009).
177. Kojima, T., Fukuda, M., Aruga, J. & Mikoshiba, K. Calcium-dependent phospholipid binding to the C2A domain of a ubiquitous form of double C2 protein (Doc2 beta). J. Biochem. 120, 671–676 (1996).
178. Davletov, B. A. & Südhof, T. C. A single C2 domain from synaptotagmin I is sufficient for high affinity Ca^{2+}/phospholipid binding. J. Biol. Chem. 268, 26386–90 (1993).
179. Suh, B.-C. & Hille, B. PIP 2 Is a Necessary Cofactor for Ion Channel Function: How and Why? Annu. Rev. Biophys. 37, 175–195 (2008).
180. Montaville, P. et al. The PIP2 binding mode of the C2 domains of rabphilin-3A. Protein Sci. 17, 1025–34 (2008).

181. de Jong, A. P. H. et al. RIM C2B Domains Target Presynaptic Active Zone Functions to PIP2-Containing Membranes. Neuron 98, 335-349.e7 (2018).
182. Martin, T. F. . PI(4,5)P2 regulation of surface membrane traffic. Curr. Opin. Cell Biol. 13, 493–499 (2001).
183. Michaeli, L., Gottfried, I., Bykhovskaia, M. & Ashery, U. Phosphatidylinositol (4, 5)-bisphosphate targets double C2 domain protein B to the plasma membrane. Traffic 18, 825–839 (2017).
184. Bradberry, M. M., Bao, H., Lou, X. & Chapman, E. R. PIP2 drives Ca^{2+}-independent membrane penetration by the tandem C2 domain proteins synaptotagmin-1 and Doc2β. J. Biol. Chem. (2019). doi:10.1074/jbc.RA119.007929
185. Manna, D. et al. Differential Roles of Phosphatidylserine, PtdIns(4,5)P 2 , and PtdIns(3,4,5)P 3 in Plasma Membrane Targeting of C2 Domains. J. Biol. Chem. 283, 26047–26058 (2008).
186. Conesa-Zamora, P., Lopez-Andreo, M. J., Gómez-Fernández, J. C. & Corbalán-García, S. Identification of the phosphatidylserine binding site in the C2 domain that is important for PKCα activation and in vivo cell localization. Biochemistry 40, 13898–13905 (2001).
187. Bai, J., Tucker, W. C. & Chapman, E. R. PIP2 increases the speed of response of synaptotagmin and steers its membrane-penetration activity toward the plasma membrane. Nat. Struct. Mol. Biol. 11, 36–44 (2004).
188. Rickman, C. et al. Synaptotagmin interaction with the syntaxin/SNAP-25 dimer is mediated by an evolutionarily conserved motif and is sensitive to inositol hexakisphosphate. J. Biol. Chem. 279, 12574–9 (2004).
189. Suh, B.-C., Inoue, T., Meyer, T. & Hille, B. Rapid chemically induced changes of PtdIns(4,5)P2 gate KCNQ ion channels. Science 314, 1454–7 (2006).
190. Hori, T., Takai, Y. & Takahashi, T. Presynaptic mechanism for phorbol ester-induced synaptic potentiation. J. Neurosci. 19, 7262–7 (1999).
191. García, R. A., Pantazatos, S. P., Pantazatos, D. P. & MacDonald, R. C. Cholesterol stabilizes hemifused phospholipid bilayer vesicles. Biochim. Biophys. Acta 1511, 264–70 (2001).
192. Tse, A., Lee, A. K., Yan, L. & Tse, F. W. Influence of cholesterol on cellular signaling and fusion pore kinetics. J. Mol. Neurosci. 48, 395–401 (2012).
193. Zhang, J., Xue, R., Ong, W.-Y. & Chen, P. Roles of cholesterol in vesicle fusion and motion. Biophys. J. 97, 1371–80 (2009).
194. Najafinobar, N. et al. Cholesterol Alters the Dynamics of Release in Protein Independent Cell Models for Exocytosis. Sci. Rep. 6, 33702 (2016).
195. Lang, T. et al. SNAREs are concentrated in cholesterol-dependent clusters that define docking and fusion sites for exocytosis. EMBO J. 20, 2202–13 (2001).
196. Chamberlain, L. H., Burgoyne, R. D. & Gould, G. W. SNARE proteins are highly enriched in lipid rafts in PC12 cells: implications for the spatial control of exocytosis. Proc. Natl. Acad. Sci. U. S. A. 98, 5619–24 (2001).
197. Low, S. H. et al. Syntaxins 3 and 4 are concentrated in separate clusters on the plasma membrane before the establishment of cell polarity. Mol. Biol. Cell 17, 977–89 (2006).
198. Chamberlain, L. H. & Gould, G. W. The vesicle- and target-SNARE proteins that mediate Glut4 vesicle fusion are localized in detergent-insoluble lipid rafts present on distinct intracellular membranes. J. Biol. Chem. 277, 49750–4 (2002).
199. Wasser, C. R., Ertunc, M., Liu, X. & Kavalali, E. T. Cholesterol-dependent balance between evoked and spontaneous synaptic vesicle recycling. J. Physiol. 579, 413–29 (2007).
200. Linetti, A. et al. Cholesterol reduction impairs exocytosis of synaptic vesicles. J. Cell Sci. 123, 595–605 (2010).
201. de Jong, A. P. & Verhage, M. Presynaptic signal transduction pathways that modulate synaptic transmission. Curr. Opin. Neurobiol. 19, 245–253 (2009).
202. Wierda, K. D. B., Toonen, R. F. G., de Wit, H., Brussaard, A. B. & Verhage, M. Interdependence of PKC-dependent and PKC-independent pathways for presynaptic plasticity. Neuron 54, 275–290 (2007).
203. de Jong, A. P. H. et al. Phosphorylation of synaptotagmin-1 controls a post-priming step in PKC-dependent presynaptic plasticity. Proc. Natl. Acad. Sci. 113, 5095–5100 (2016).
204. Groffen, A. J. A. et al. Ca^{2+}-induced recruitment of the secretory vesicle protein DOC2B to the target membrane. J. Biol. Chem. 279, 23740–23747 (2004).
205. Bootman, M. D. Calcium signaling. Cold Spring Harb. Perspect. Biol. 4, a011171 (2012).
206. Risselada, H. J. & Grubmüller, H. How SNARE molecules mediate membrane fusion: Recent insights from molecular simulations. Curr. Opin. Struct. Biol. 22, 187–196 (2012).
207. Sorkin, R. et al. Synaptotagmin-1 and Doc2b Exhibit Distinct Membrane-Remodeling Mechanisms. Biophys. J. 118, 643–656 (2020).
208. Brouwer, I. et al. Direct quantitative detection of Doc2b-induced hemifusion in optically trapped membranes. Nat. Commun. 6, 8387 (2015).
209. Connell, E. et al. Cross-linking of Phospholipid Membranes is a Conserved Property of Calcium-sensitive Synaptotagmins. J. Mol. Biol. 380, 42–50 (2008).

210. Boyman, L., Mikhasenko, H., Hiller, R. & Khananshvili, D. Kinetic and equilibrium properties of regulatory calcium sensors of NCX1 protein. J. Biol. Chem. 284, 6185–93 (2009).
211. Striegel, A. R. et al. Calcium binding by synaptotagmin's C2A domain is an essential element of the electrostatic switch that triggers synchronous synaptic transmission. J. Neurosci. 32, 1253–1260 (2012).
212. Ubach, J., García, J., Nittler, M. P., Südhof, T. C. & Rizo, J. Structure of the Janus-faced C2B domain of rabphilin. Nat. Cell Biol. 1, 106–12 (1999).
213. Muravyov, A. et al. Calcium signaling. Cold Spring Perspect. Biol. 740, 1–4 (2012).
214. Berridge, M. J. Neuronal calcium signaling. Neuron 21, 13–26 (1998).
215. Helmchen, F., Borst, J. G. & Sakmann, B. Calcium dynamics associated with a single action potential in a CNS presynaptic terminal. Biophys. J. 72, 1458–71 (1997).
216. Maravall, M., Mainen, Z. F., Sabatini, B. L. & Svoboda, K. Estimating intracellular calcium concentrations and buffering without wavelength ratioing. Biophys. J. 78, 2655–2667 (2000).
217. Sabatini, B. L., Oertner, T. G. & Svoboda, K. The life cycle of Ca^{2+} ions in dendritic spines. Neuron 33, 439–452 (2002).
218. Scott, R. & Rusakov, D. A. Main determinants of presynaptic Ca^{2+} dynamics at individual mossy fiber-CA3 pyramidal cell synapses. J Neurosci 26, 7071–7081 (2006).
219. Bollmann, J. H., Sakmann, B. & Borst, J. G. Calcium sensitivity of glutamate release in a calyx-type terminal. Science 289, 953–7 (2000).
220. Schneggenburger, R. & Neher, E. Intracellular calcium dependence of transmitter release rates at a fast central synapse. Nature 406, 889–93 (2000).
221. Lou, X., Scheuss, V. & Schneggenburger, R. Allosteric modulation of the presynaptic Ca^{2+} sensor for vesicle fusion. Nature 435, 497–501 (2005).
222. Clapham, D. E. Calcium Signaling. Cell 131, 1047–1058 (2007).
223. MacDermott, A. B., Role, L. W. & Siegelbaum, S. A. Presynaptic ionotropic receptors and the control of transmitter release. Annu. Rev. Neurosci. 22, 443–85 (1999).
224. Koester, H. J. & Sakmann, B. Calcium dynamics associated with action potentials in single nerve terminals of pyramidal cells in layer 2/3 of the young rat neocortex. J. Physiol. 529 Pt 3, 625–46 (2000).
225. Meinrenken, C. J., Borst, J. G. G. & Sakmann, B. Calcium secretion coupling at calyx of Held governed by nonuniform channel-vesicle topography. J. Neurosci. 22, 1648–67 (2002).
226. Dietrich, D. et al. Functional specialization of presynaptic Cav2.3 Ca^{2+} channels. Neuron 39, 483–96 (2003).
227. Berridge, M. J. Calcium microdomains: organization and function. Cell Calcium 40, 405–12 (2006).
228. Stanley, E. F. The calcium channel and the organization of the presynaptic transmitter release face. Trends Neurosci. 20, 404–9 (1997).
229. Miller, R. J. Multiple calcium channels and neuronal function. Science 235, 46–52 (1987).
230. Kerr, L. M. & Yoshikami, D. A venom peptide with a novel presynaptic blocking action. Nature 308, 282–4 (1984).
231. Dunlap, K., Luebke, J. I. & Turner, T. J. Exocytotic Ca^{2+} channels in mammalian central neurons. Trends Neurosci. 18, 89–98 (1995).
232. Rettig, J. et al. Isoform-specific interaction of the alpha1A subunits of brain Ca^{2+} channels with the presynaptic proteins syntaxin and SNAP-25. Proc. Natl. Acad. Sci. U. S. A. 93, 7363–8 (1996).
233. Charvin, N. et al. Direct interaction of the calcium sensor protein synaptotagmin I with a cytoplasmic domain of the alpha1A subunit of the P/Q-type calcium channel. EMBO J. 16, 4591–6 (1997).
234. Catterall, W. A. Voltage-gated calcium channels. Cold Spring Harb. Perspect. Biol. 3, a003947 (2011).
235. Joseph, S. K., Brownell, S. & Khan, M. T. Calcium regulation of inositol 1,4,5-trisphosphate receptors. Cell Calcium 38, 539–46 (2005).
236. Verkhratsky, A. & Shmigol, A. Calcium-induced calcium release in neurones. Cell Calcium 19, 1–14 (1996).
237. Emptage, N. J., Reid, C. A. & Fine, A. Calcium stores in hippocampal synaptic boutons mediate short-term plasticity, store-operated Ca^{2+} entry, and spontaneous transmitter release. Neuron 29, 197–208 (2001).
238. Llano, I. et al. Presynaptic calcium stores underlie large-amplitude miniature IPSCs and spontaneous calcium transients. Nat. Neurosci. 3, 1256–1265 (2000).
239. Bardo, S., Cavazzini, M. G. & Emptage, N. The role of the endoplasmic reticulum Ca^{2+} store in the plasticity of central neurons. Trends Pharmacol. Sci. 27, 78–84 (2006).
240. Carter, A. G., Vogt, K. E., Foster, K. A. & Regehr, W. G. Assessing the Role of Calcium-Induced Calcium Release in Short-Term Presynaptic Plasticity at Excitatory Central Synapses. J. Neurosci. 22, 21–28 (2002).
241. Ermolyuk, Y. S. et al. Differential triggering of spontaneous glutamate release by P/Q-, N- and R-type Ca^{2+} channels. Nat. Neurosci. 16, 1754–1763 (2013).
242. Simkus, C. R. L. & Stricker, C. The contribution of intracellular calcium stores to mEPSCs recorded in layer II

neurones of rat barrel cortex. J. Physiol. 545, 521–535 (2002).
243. Reese, A. L. & Kavalali, E. T. Spontaneous neurotransmission signals through store-driven Ca(2+) transients to maintain synaptic homeostasis. Elife 4, 1–15 (2015).
244. Lefkowitz, J. J. et al. Suppression of Ca^{2+} syntillas increases spontaneous exocytosis in mouse adrenal chromaffin cells. J. Gen. Physiol. 134, 267–80 (2009).
245. Quinlan, M. E., Alberto, C. O. & Hirasawa, M. Short-term potentiation of mEPSCs requires N-, P/Q- and L-type Ca^{2+} channels and mitochondria in the supraoptic nucleus. J. Physiol. 586, 3147–61 (2008).
246. De Crescenzo, V. et al. Ca^{2+} syntillas, miniature Ca^{2+} release events in terminals of hypothalamic neurons, are increased in frequency by depolarization in the absence of Ca^{2+} influx. J. Neurosci. 24, 1226–35 (2004).
247. Koizumi, S. et al. Characterization of elementary Ca^{2+} release signals in NGF-differentiated PC12 cells and hippocampal neurons. Neuron 22, 125–137 (1999).
248. Vassilatis, D. K. et al. The G protein-coupled receptor repertoires of human and mouse. Proc. Natl. Acad. Sci. U. S. A. 100, 4903–8 (2003).
249. Zeng, W. et al. A New Mode of Ca^{2+} Signaling by G Protein-Coupled Receptors. Curr. Biol. 13, 872–876 (2003).
250. Berridge, M. J. Inositol trisphosphate and calcium signalling. Nature 361, 315–325 (1993).
251. Manita, S. & Ross, W. N. Synaptic activation and membrane potential changes modulate the frequency of spontaneous elementary Ca^{2+} release events in the dendrites of pyramidal neurons. J. Neurosci. 29, 7833–45 (2009).
252. Ross, W. N. Understanding calcium waves and sparks in central neurons. Nat. Rev. Neurosci. 13, 157–68 (2012).
253. Vyleta, N. P. & Smith, S. M. Spontaneous glutamate release is independent of calcium influx and tonically activated by the calcium-sensing receptor. J. Neurosci. 31, 4593–4606 (2011).
254. Terasaki, M., Slater, N. T., Fein, A., Schmidek, A. & Reese, T. S. Continuous network of endoplasmic reticulum in cerebellar Purkinje neurons. Proc. Natl. Acad. Sci. 91, 7510–7514 (1994).
255. Terasaki, M. et al. Stacked Endoplasmic Reticulum Sheets Are Connected by Helicoidal Membrane Motifs. Cell 154, 285–296 (2013).
256. Tsukita, S. & Ishikawa, H. THREE-DIMENSIONAL DISTRIBUTIONOF SMOOTH ENDOPLASMIC RETICULUM IN MYELINATED AXONS. J. Electron Microsc. (Tokyo). (1976). doi:10.1093/oxfordjournals.jmicro.a050013
257. Terasaki, M. Axonal endoplasmic reticulum is very narrow. J. Cell Sci. 131, jcs210450 (2018).
258. Karagas, N. E. & Venkatachalam, K. Roles for the Endoplasmic Reticulum in Regulation of Neuronal Calcium Homeostasis. Cells 8, 1232 (2019).
259. Shepherd, G. M. G. & Harris, K. M. Three-Dimensional Structure and Composition of CA3→CA1 Axons in Rat Hippocampal Slices: Implications for Presynaptic Connectivity and Compartmentalization. J. Neurosci. 18, 8300–8310 (1998).
260. Benedeczky, I., Molnár, E. & Somogyi, P. The cisternal organelle as a Ca^{2+}-storing compartment associated with GABAergic synapses in the axon initial segment of hippocampal pyramidal neurones. Exp. Brain Res. 101, 216–230 (1994).
261. Bartol, T. M. et al. Computational reconstitution of spine calcium transients from individual proteins. Front. Synaptic Neurosci. 7, (2015).
262. Wu, Y. et al. Contacts between the endoplasmic reticulum and other membranes in neurons. Proc. Natl. Acad. Sci. 114, E4859–E4867 (2017).
263. Bouchard, R., Pattarini, R. & Geiger, J. D. Presence and functional significance of presynaptic ryanodine receptors. Prog. Neurobiol. 69, 391–418 (2003).
264. Ouyang, K. et al. Ca^{2+} sparks and secretion in dorsal root ganglion neurons. Proc. Natl. Acad. Sci. U. S. A. 102, 12259–64 (2005).
265. Foskett, J. K., White, C., Cheung, K.-H. & Mak, D.-O. D. Inositol Trisphosphate Receptor Ca^{2+} Release Channels. Physiol. Rev. 87, 593–658 (2007).
266. Michikawa, T. et al. Calmodulin Mediates Calcium-Dependent Inactivation of the Cerebellar Type 1 Inositol 1,4,5-Trisphosphate Receptor. Neuron 23, 799–808 (1999).
267. Williams, A. J. Ion conduction and discrimination in the sarcoplasmic reticulum ryanodine receptor/calcium-release channel. J. Muscle Res. Cell Motil. 13, 7–26 (1992).
268. Williams, A. J., West, D. J. & Sitsapesan, R. Light at the end of the Ca(2+)-release channel tunnel: structures and mechanisms involved in ion translocation in ryanodine receptor channels. Q. Rev. Biophys. 34, 61–104 (2001).
269. Meissner, G. The structural basis of ryanodine receptor ion channel function. J. Gen. Physiol. 149, 1065–1089 (2017).
270. Mataragka, S. & Taylor, C. W. All three IP 3 receptor subtypes generate Ca^{2+} puffs, the universal building blocks of IP 3 -evoked Ca^{2+} signals. J. Cell Sci. 131, jcs220848 (2018).
271. Cheng, H. & Lederer, W. J. Calcium sparks. Physiol. Rev. 88, 1491–545 (2008).

272. Cheng, H., Lederer, W. J. & Cannell, M. B. Calcium sparks: elementary events underlying excitation-contraction coupling in heart muscle. Science 262, 740–4 (1993).
273. Tsien, R. W., Lipscombe, D., Madison, D. V, Bley, K. R. & Fox, A. P. Multiple types of neuronal calcium channels and their selective modulation. Trends Neurosci. 11, 431–8 (1988).
274. Williams, C. L. & Smith, S. M. Calcium dependence of spontaneous neurotransmitter release. J. Neurosci. Res. 96, 335–347 (2018).
275. Paredes, R. M., Etzler, J. C., Watts, L. T., Zheng, W. & Lechleiter, J. D. Chemical calcium indicators. Methods 46, 143–51 (2008).
276. Whitaker, M. Genetically-encoded probes for measurement of intracellular calcium. Methods Cell Biol. 99, 153–182 (2010).
277. Hendel, T. et al. Fluorescence changes of genetic calcium indicators and OGB-1 correlated with neural activity and calcium in vivo and in vitro. J. Neurosci. 28, 7399–411 (2008).
278. Nagai, T., Sawano, A., Park, E. S. & Miyawaki, A. Circularly permuted green fluorescent proteins engineered to sense Ca^{2+}. Proc. Natl. Acad. Sci. U. S. A. 98, 3197–3202 (2001).
279. Akerboom, J. et al. Optimization of a GCaMP Calcium Indicator for Neural Activity Imaging. J. Neurosci. 32, 13819–13840 (2012).
280. Horikawa, K. Recent progress in the development of genetically encoded Ca^{2+} indicators. J. Med. Investig. 62, 24–8 (2015).
281. Mao, T., O'Connor, D. H., Scheuss, V., Nakai, J. & Svoboda, K. Characterization and subcellular targeting of GCaMP-type genetically-encoded calcium indicators. PLoS One 3, 1–10 (2008).
282. Chen, T.-W. et al. Ultrasensitive fluorescent proteins for imaging neuronal activity. Nature 499, 295–300 (2013).
283. Zhao, Y. et al. An expanded palette of genetically encoded Ca^{2+} indicators. Science 333, 1888–91 (2011).
284. Akerboom, J. et al. Genetically encoded calcium indicators for multi-color neural activity imaging and combination with optogenetics. Front. Mol. Neurosci. 6, 2 (2013).
285. Mank, M. et al. A genetically encoded calcium indicator for chronic in vivo two-photon imaging. Nat. Methods 5, 805–11 (2008).
286. Tian, L. et al. Imaging neural activity in worms, flies and mice with improved GCaMP calcium indicators. Nat. Methods 6, 875–81 (2009).
287. Grienberger, C. & Konnerth, A. Imaging calcium in neurons. Neuron 73, 862–85 (2012).
288. Davis, G. W. & Müller, M. Homeostatic Control of Presynaptic Neurotransmitter Release. Annu. Rev. Physiol. 77, 251–270 (2015).
289. Gaviño, M. A., Ford, K. J., Archila, S. & Davis, G. W. Homeostatic synaptic depression is achieved through a regulated decrease in presynaptic calcium channel abundance. Elife 4, (2015).
290. Zhao, C., Dreosti, E. & Lagnado, L. Homeostatic Synaptic Plasticity through Changes in Presynaptic Calcium Influx. J. Neurosci. 31, 7492–7496 (2011).
291. De Gois, S. Homeostatic Scaling of Vesicular Glutamate and GABA Transporter Expression in Rat Neocortical Circuits. J. Neurosci. 25, 7121–7133 (2005).
292. Delvendahl, I. & Müller, M. Homeostatic plasticity—a presynaptic perspective. Curr. Opin. Neurobiol. 54, 155–162 (2019).
293. Kandel, E. R. The molecular biology of memory storage: a dialogue between genes and synapses. Science 294, 1030–8 (2001).
294. Fusi, S., Drew, P. J. & Abbott, L. F. Cascade Models of Synaptically Stored Memories. Neuron 45, 599–611 (2005).
295. Yang, Y. & Calakos, N. Presynaptic long-term plasticity. Front. Synaptic Neurosci. 5, (2013).
296. Ehlers, M. D., Heine, M., Groc, L., Lee, M.-C. & Choquet, D. Diffusional trapping of GluR1 AMPA receptors by input-specific synaptic activity. Neuron 54, 447–60 (2007).
297. Jourdain, P. et al. Glutamate exocytosis from astrocytes controls synaptic strength. Nat. Neurosci. 10, 331–9 (2007).
298. Savtchouk, I. et al. Circuit-specific control of the medial entorhinal inputs to the dentate gyrus by atypical presynaptic NMDARs activated by astrocytes. Proc. Natl. Acad. Sci. U. S. A. 116, 13602–13610 (2019).
299. Monday, H. R., Younts, T. J. & Castillo, P. E. Long-Term Plasticity of Neurotransmitter Release: Emerging Mechanisms and Contributions to Brain Function and Disease. Annu. Rev. Neurosci. 41, 299–322 (2018).
300. Jackman, S. L. & Regehr, W. G. The Mechanisms and Functions of Synaptic Facilitation. Neuron 94, 447–464 (2017).
301. Rebola, N., Carta, M. & Mulle, C. Operation and plasticity of hippocampal CA3 circuits: implications for memory encoding. Nat. Rev. Neurosci. 18, 208–220 (2017).
302. Nicoll, R. A. & Schmitz, D. Synaptic plasticity at hippocampal mossy fibre synapses. Nat. Rev. Neurosci. 6,

863–876 (2005).
303. Deng, P.-Y. & Klyachko, V. A. The diverse functions of short-term plasticity components in synaptic computations. Commun. Integr. Biol. 4, 543–8 (2011).
304. Klyachko, V. A. & Stevens, C. F. Excitatory and feed-forward inhibitory hippocampal synapses work synergistically as an adaptive filter of natural spike trains. PLoS Biol. 4, e207 (2006).
305. Chung, S., Li, X. & Nelson, S. B. Short-term depression at thalamocortical synapses contributes to rapid adaptation of cortical sensory responses in vivo. Neuron 34, 437–46 (2002).
306. Cook, D. L., Schwindt, P. C., Grande, L. A. & Spain, W. J. Synaptic depression in the localization of sound. Nature 421, 66–70 (2003).
307. Nanou, E., Sullivan, J. M., Scheuer, T. & Catterall, W. A. Calcium sensor regulation of the CaV2.1 Ca^{2+} channel contributes to short-term synaptic plasticity in hippocampal neurons. Proc. Natl. Acad. Sci. U. S. A. 113, 1062–7 (2016).
308. Matveev, V. Ca^{2+}buffering as a mechanism of short-term synaptic plasticity. BMC Neurosci. 14, P269 (2013).
309. Ariel, P., Hoppa, M. B. & Ryan, T. A. Intrinsic variability in Pv, RRP size, $Ca^{(2+)}$ channel repertoire, and presynaptic potentiation in individual synaptic boutons. Front. Synaptic Neurosci. 4, 9 (2012).
310. Habets, R. L. P. & Borst, J. G. G. Dynamics of the readily releasable pool during post-tetanic potentiation in the rat calyx of Held synapse. J. Physiol. 581, 467–78 (2007).
311. Delaney, K. R., Zucker, R. S. & Tank, D. W. Calcium in motor nerve terminals associated with posttetanic potentiation. J. Neurosci. 9, 3558–67 (1989).
312. Delaney, K. R. & Tank, D. W. A quantitative measurement of the dependence of short-term synaptic enhancement on presynaptic residual calcium. J. Neurosci. 14, 5885–902 (1994).
313. Regehr, W. G., Delaney, K. R. & Tank, D. W. The role of presynaptic calcium in short-term enhancement at the hippocampal mossy fiber synapse. J. Neurosci. 14, 523–37 (1994).
314. Neher, E. & Sakaba, T. Multiple roles of calcium ions in the regulation of neurotransmitter release. Neuron 59, 861–72 (2008).
315. Regehr, W. G. Short-term presynaptic plasticity. Cold Spring Harb. Perspect. Biol. 4, a005702 (2012).
316. Schneggenburger, R., Sakaba, T. & Neher, E. Vesicle pools and short-term synaptic depression: lessons from a large synapse. Trends Neurosci. 25, 206–12 (2002).
317. Müller, M., Goutman, J. D., Kochubey, O. & Schneggenburger, R. Interaction between facilitation and depression at a large CNS synapse reveals mechanisms of short-term plasticity. J. Neurosci. 30, 2007–16 (2010).
318. Dittman, J. S., Kreitzer, A. C. & Regehr, W. G. Interplay between facilitation, depression, and residual calcium at three presynaptic terminals. J. Neurosci. 20, 1374–85 (2000).
319. Rosenmund, C., Clements, J. & Westbrook, G. Nonuniform probability of glutamate release at a hippocampal synapse. Science (80-.). 262, 754–757 (1993).
320. Hanse, E. & Gustafsson, B. Vesicle release probability and pre-primed pool at glutamatergic synapses in area CA1 of the rat neonatal hippocampus. J. Physiol. 531, 481–493 (2001).
321. Murthy, V. N., Sejnowski, T. J. & Stevens, C. F. Heterogeneous Release Properties of Visualized Individual Hippocampal Synapses. Neuron 18, 599–612 (1997).
322. Burnashev, N. & Rozov, A. Presynaptic Ca^{2+} dynamics, Ca^{2+} buffers and synaptic efficacy. Cell Calcium 37, 489–95 (2005).
323. Yamada, W. M. & Zucker, R. S. Time course of transmitter release calculated from simulations of a calcium diffusion model. Biophys. J. 61, 671–82 (1992).
324. Xue, R. et al. Doc2-mediated superpriming supports synaptic augmentation. Proc. Natl. Acad. Sci. U. S. A. 115, E5605–E5613 (2018).
325. Lin, Y. Q., Brain, K. L. & Bennett, M. R. Calcium in sympathetic boutons of rat superior cervical ganglion during facilitation, augmentation and potentiation. J. Auton. Nerv. Syst. 73, 26–37 (1998).
326. Mochida, S., Few, A. P., Scheuer, T. & Catterall, W. A. Regulation of presynaptic Ca(V)2.1 channels by Ca^{2+} sensor proteins mediates short-term synaptic plasticity. Neuron 57, 210–6 (2008).
327. Korogod, N., Lou, X. & Schneggenburger, R. Posttetanic potentiation critically depends on an enhanced $Ca^{(2+)}$ sensitivity of vesicle fusion mediated by presynaptic PKC. Proc. Natl. Acad. Sci. U. S. A. 104, 15923–8 (2007).
328. Habets, R. L. P. & Borst, J. G. G. An increase in calcium influx contributes to post-tetanic potentiation at the rat calyx of Held synapse. J. Neurophysiol. 96, 2868–76 (2006).
329. Borst, J. G. & Sakmann, B. Depletion of calcium in the synaptic cleft of a calyx-type synapse in the rat brainstem. J. Physiol. 521 Pt 1, 123–33 (1999).
330. Katsuki, H., Izumi, Y. & Zorumski, C. F. Removal of extracellular calcium after conditioning stimulation disrupts long-term potentiation in the CA1 region of rat hippocampal slices. Neuroscience 76, 1113–9 (1997).
331. Wang, L. Y. & Kaczmarek, L. K. High-frequency firing helps replenish the readily releasable pool of synaptic

vesicles. Nature 394, 384–8 (1998).
332. Alle, H., Jonas, P. & Geiger, J. R. PTP and LTP at a hippocampal mossy fiber-interneuron synapse. Proc. Natl. Acad. Sci. U. S. A. 98, 14708–13 (2001).
333. Brager, D. H., Cai, X. & Thompson, S. M. Activity-dependent activation of presynaptic protein kinase C mediates post-tetanic potentiation. Nat. Neurosci. 6, 551–2 (2003).
334. Fioravante, D., Chu, Y., Myoga, M. H., Leitges, M. & Regehr, W. G. Calcium-dependent isoforms of protein kinase C mediate posttetanic potentiation at the calyx of Held. Neuron 70, 1005–19 (2011).
335. Micheva, K. D., Holz, R. W. & Smith, S. J. Regulation of presynaptic phosphatidylinositol 4,5-biphosphate by neuronal activity. J. Cell Biol. 154, 355–68 (2001).
336. Barclay, J. W. et al. Phosphorylation of Munc18 by Protein Kinase C Regulates the Kinetics of Exocytosis. J. Biol. Chem. 278, 10538–10545 (2003).
337. Lipstein, N. et al. Dynamic control of synaptic vesicle replenishment and short-term plasticity by $Ca^{(2+)}$-calmodulin-Munc13-1 signaling. Neuron 79, 82–96 (2013).
338. Rosenmund, C. et al. Differential control of vesicle priming and short-term plasticity by Munc13 isoforms. Neuron 33, 411–24 (2002).
339. Rhee, J. S. et al. Beta phorbol ester- and diacylglycerol-induced augmentation of transmitter release is mediated by Munc13s and not by PKCs. Cell 108, 121–33 (2002).
340. Duncan, R. R., Betz, A., Shipston, M. J., Brose, N. & Chow, R. H. Transient, phorbol ester-induced DOC2-Munc13 interactions in vivo. J. Biol. Chem. 274, 27347–27350 (1999).
341. Habets, R. L. P. & Borst, J. G. G. Post-tetanic potentiation in the rat calyx of Held synapse. J. Physiol. 564, 173–87 (2005).